



# Evaluation of Aerial LiDAR Surveys for Resource Road Engineering: A Case Study in Coastal British Columbia

**Date: October 2015 – Technical Report No. 50**

**By:**

Matt Kurowski, MSc, EIT, Researcher, Resource Roads

**Non-Restricted to Members and  
Partners of FPInnovations**



FPInnovations is a not-for-profit world-leading R&D institute that specializes in the creation of scientific solutions in support of the Canadian forest sector's global competitiveness and responds to the priority needs of its industry members and government partners. It is ideally positioned to perform research, innovate, and deliver state-of-the-art solutions for every area of the sector's value chain, from forest operations to consumer and industrial products. FPInnovations' staff numbers more than 525. Its R&D laboratories are located in Québec City, Montréal and Vancouver, and it has technology transfer offices across Canada. For more information about FPInnovations, visit: [www.fpinnovations.ca](http://www.fpinnovations.ca).

Follow us on:  

301010078: 1.4.1 EFI 60K  
TECHNICAL REPORT – T50

## ACKNOWLEDGEMENTS

This project was financially supported by the Canadian Wood Fibre Centre (Natural Resources Canada–Canadian Forest Service) under its contribution agreement with FPInnovations. The British Columbia Ministry of Forests, Lands and Natural Resource Operations also made in-kind contributions for field work.

## REVIEWERS

Allan Bradley, RPF, PEng  
Associate Program Leader, Resource Roads  
FPInnovations

Brian Chow, PEng  
Chief Engineer, British Columbia Ministry of  
Forests, Lands and Natural Resource Operations

## CONTACT

Matt Kurowski, Msc, EIT  
Researcher, Resource Roads  
FPInnovations  
604.222.5727  
[matt.kurowski@fpinnovations.ca](mailto:matt.kurowski@fpinnovations.ca)

© 2015 FPInnovations. All rights reserved. Unauthorized copying or redistribution prohibited.

Disclosure for Commercial Application: If you require assistance to implement these research findings, please contact FPInnovations at [info@fpinnovations.ca](mailto:info@fpinnovations.ca).

## Table of contents

Executive Summary .....	7
Introduction.....	7
Review of Available datasets and Accuracy terminology.....	8
Study Location .....	8
Data Collection and Post-Processing .....	8
LiDAR and LiDAR-Derived Data Files .....	9
Imagery Data Files .....	11
Accuracy of the LiDAR and LiDAR-Derived Datasets .....	12
Use of Checkpoints .....	13
Absolute Accuracy Reporting .....	15
Relative Accuracy Reporting .....	17
Field Methods .....	17
Constraints in Using GNSS to Check LiDAR Accuracy.....	17
Field Work.....	18
First Field Visit.....	18
Second Field Visit.....	20
Processing the Data from the First Field Visit .....	20
Second Field Visit.....	22
Processing of the Data from the Second Field Visit .....	23
Post-Survey Breaklines .....	25
Evaluation of Accuracy .....	25
Data Preparation .....	26
Selecting a Reference Terrain Model.....	26
Filtering Points by Horizontal Proximity.....	26
Making Slope and Canopy Raster Layers.....	27
Differences Between LiDAR and Ground-Survey Terrain Models.....	27
Summary and Discussion of Vertical Accuracy Results.....	33
Effects of Post-Survey Breaklines on Earthworks Calculations.....	34
Summary and Discussion of the Effects of Post-Survey Breaklines in DEM Production.....	35
Cut-and-Fill Differences Using LiDAR Versus Conventional Terrain Models .....	36
Summary and Discussion for Earthworks Analysis .....	37
Overall Benefits and Limitations of LiDAR.....	38

Benefits .....	38
Limitations .....	39
Conclusions .....	41
References .....	43

## List of Figures

Figure 1: Map of the In-SHUCK-ch FSR..	9
Figure 2: Two close-up 3D views of the same area along the In-SHUCK-ch FSR.....	10
Figure 3: DEM image files.....	11
Figure 4: A comparison of two images obtained from different files .....	12
Figure 5: Control points .....	13
Figure 6: Two 10-cm orthophotos showing checkpoints.....	14
Figure 7: Georeferencing field equipment. ....	19
Figure 8: Two examples of the types of survey markers encountered on the In-SHUCK-ch FSR.....	20
Figure 9: Close-ups of conventional surveyors at Road Section A and Road Section B.....	22
Figure 10: Four representations of Road Subsection A3.....	24
Figure 11: Close-up view of breaklines in Road Section A. ....	25
Figure 12: Close-up of Road Section A.....	27
Figure 13: Error distribution and frequency associated with LiDAR data, for flat terrain with open sky, where flat is defined as $\leq 3$ degrees slope. ....	29
Figure 14: Error distribution and frequency associated with LiDAR data, for flat terrain with canopy in Road Section A, where flat is defined as $\leq 6$ degrees slope.....	30
Figure 15: Error distribution and frequency associated with LiDAR data, for flat terrain with open sky, where flat is defined as $\leq 6$ degrees slope. ....	31
Figure 16: Error distribution and frequency associated with LiDAR data, for steep terrain with canopy in Road Section A, where steep is defined as $>25\%$ slope. ....	32
Figure 17: A difference raster for the first kilometer of Road Section A .....	35
Figure 18: Example of how slope-stake locations vary with the ground model. ....	36

**List of tables**

Table 1. Summary of vertical checkpoints..... 15

Table 2: Road subsections where detailed total station surveys were completed..... 23

Table 3: Accuracy associated with LiDAR data, for flat terrain with open sky, where flat is defined as  $\leq 3\%$  slope..... 33

Table 4: Accuracy associated with LiDAR data, for flat terrain with open sky, where flat is defined as  $\leq 6\%$  slope..... 33

Table 5: Accuracy associated with LiDAR data, for flat terrain with canopy, steep terrain with open sky, and steep terrain with canopy, where flat is defined as  $< 6$ -degree slope, and steep as  $> 25\%$  slope.... 33

Table 6: Estimated earthworks volumes for Road Sections A and B: a comparison of calculations by model..... 37

Table 7: Estimated earthworks volumes at three road subsections..... 37

## EXECUTIVE SUMMARY

At the request of the British Columbia Ministry of Forests, Lands and Natural Resource Operations (FLNRO), in 2014 FPIInnovations evaluated the advantages and limitations of using as-built surveys derived from aerial LiDAR to inform resource road re-alignment designs.

In order to study the accuracy of LiDAR, FPIInnovations undertook a case study at the In-SHUCK-ch Forest Service Road (FSR), which is located ~150 km east–northeast of Vancouver, British Columbia, in the coastal mountains. FNLRO had recently purchased a 74-km-long, 500-m-wide strip of aerial LiDAR data for this FSR to assist in the surveying of a multi-year road upgrade project. Within this strip, two existing conventional as-built surveys were georeferenced and then utilized to evaluate the accuracy of LiDAR under different terrain conditions. Both the LiDAR and ground survey terrain models were used to design re-aligned road sections in order to compare earthworks calculations.

The main advantage of using LiDAR rather than the conventional ground survey approach is its efficiency; however, the accuracy of LiDAR is influenced by terrain features including canopy and slope, and accuracy also relies on the proprietary algorithms of LiDAR vendors to correctly identify points as ground or vegetation. In flat terrain conditions where there was also open sky, the accuracy of LiDAR was found to conform to the LiDAR vendor's specifications. As expected, accuracy progressively worsened in flat terrain with canopy, sloped terrain with open sky, and sloped terrain with canopy. While some statistically significant over and under estimations were found within these conditions, the errors were relatively small from the perspective of resource road engineering.

The earthworks calculations associated with terrain models based on LiDAR and ground surveys were found to differ between –15 and 22%. Since no survey existed that exceeded the accuracy of the conventional or LiDAR surveys, a detailed ground survey was also conducted along six small subsections of the road, where LiDAR proved to be at least as good or better in predicting earthworks volumes.

The cumulative results from the quantitative analyses of this study indicated that LiDAR was the better surveying approach. Other advantages of LiDAR are that less field work is needed if re-alignment involves planning any new road through portions of forest, its accuracy can be checked much more readily than conventional surveys, and the cost of LiDAR is much less if the survey area is large enough.

Relevant limitations of using LiDAR for engineering design of forest roads include that its ground point density can be sparse under canopy, its accuracy fluctuates with terrain conditions and can include some over and under estimation, it requires expensive equipment to tie-in from the ground, and it requires an upfront investment to acquire the survey data.

## INTRODUCTION

A major advantage of purchasing aerial LiDAR data is that a cost-effective digital terrain model (DTM) can be produced from it that can support a multitude of planning-scale tasks. It is further possible to leverage the DTM for road design, including forest resource roads; however, at larger scales, accuracy and precision errors become relevant, and thus the model may not meet certain engineering standards.

The most error-prone areas of a forestland DTM typically have steep, rough terrain and/or canopy cover. Within these terrain types, a DTM has significantly less precision compared to open, flat areas, and it also has potential to be biased or contain inaccuracies. Less precision relates to the occurrence of more fluctuation in elevation estimates, and inaccuracy could result if the average elevation of the DTM is significantly different from ground truth. Understanding these accuracy limitations for aerial LiDAR, along with the technology required to tie-in to this type of survey, is fundamental to investing in the technology—especially if the primary use is for road design.

The British Columbia Ministry of Forests, Land and Natural Resource Operations (FLNRO) requested FPInnovations to evaluate the benefits and limitations of using aerial LiDAR for resource road re-alignment upgrades. To address this need, in 2014 FPInnovations developed a case study of the In-SHUCK-ch Forest Service Road (FSR), where FLNRO had recently purchased a 74-km-long and 500-m-wide strip of aerial LiDAR and orthophotos to support a multi-year road upgrade project.

This report first expands upon the data delivered by the LiDAR vendor and clarifies the associated LiDAR accuracy-reporting techniques. Next, it reviews the field work methods used to evaluate the accuracy of the LiDAR dataset and then reviews accuracy assessment results. Finally, it examines how LiDAR affected earthworks volumes for a road re-alignment relative to using ground-based DTMs. Based on the outcomes of the case study this report discusses the overall benefits and limitations of using aerial LiDAR for resource road re-alignment.

## REVIEW OF AVAILABLE DATASETS AND ACCURACY TERMINOLOGY

### Study Location

The In-SHUCK-ch FSR is located approximately 150 km east–northeast of Vancouver, British Columbia in the coastal mountains. The northern end of the FSR (KM 0) is located just south of the town of Pemberton, at the junction of the Lillooet Lake Road and the Duffy Lake Road (both of which are parts of Highway 99). The FSR extends 74 km southwards, following the eastern shore of Lillooet Lake and Lillooet River until it ends at the north end of Harrison Lake (KM 74). The FSR provides access to First Nation and other communities along the Lillooett Lake and Lillooett River.

### Data Collection and Post-Processing

An aerial survey contractor working for FLNRO collected LiDAR and imagery along the In-SCHUCK-ch FSR on August 7<sup>th</sup> and 8<sup>th</sup>, 2013. The contractor delivered the post-processed datasets to FLNRO approximately 10 weeks later.

To keep the sizes of the delivered files manageable, the data were split up into 107 tiles, with each tile covering an area of 1x1 km (Figure 1, delivered as a .dwg and a .kml file). The linear referencing system starts at the north end of the road (KM 0 on the FSR) and ends at the south end (KM 74).

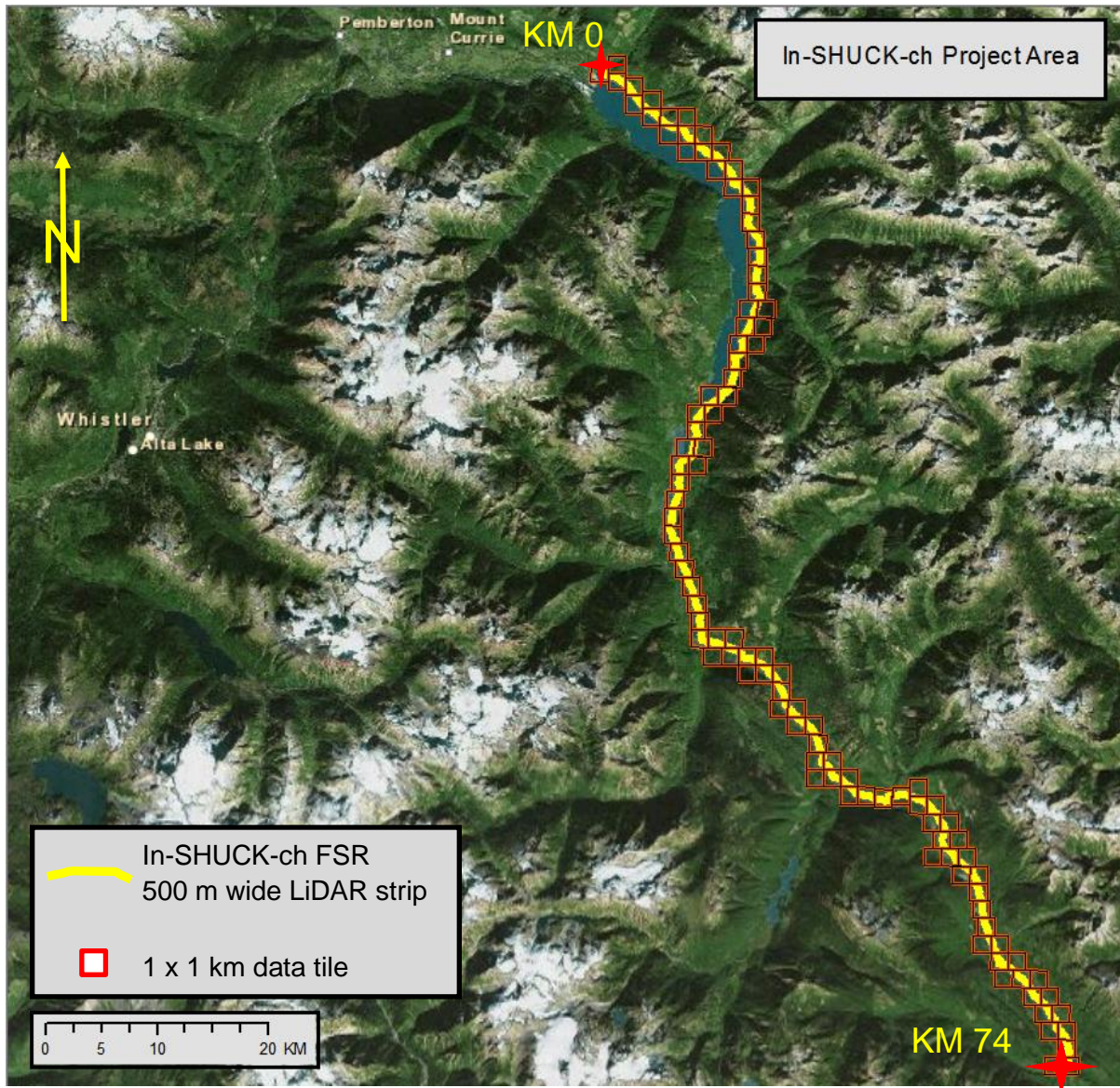


Figure 1: Map of the In-SHUCK-ch FSR. The northern end of the 74-km-long road is located in the coastal mountains, ~150 km east–northeast of Vancouver, British Columbia.

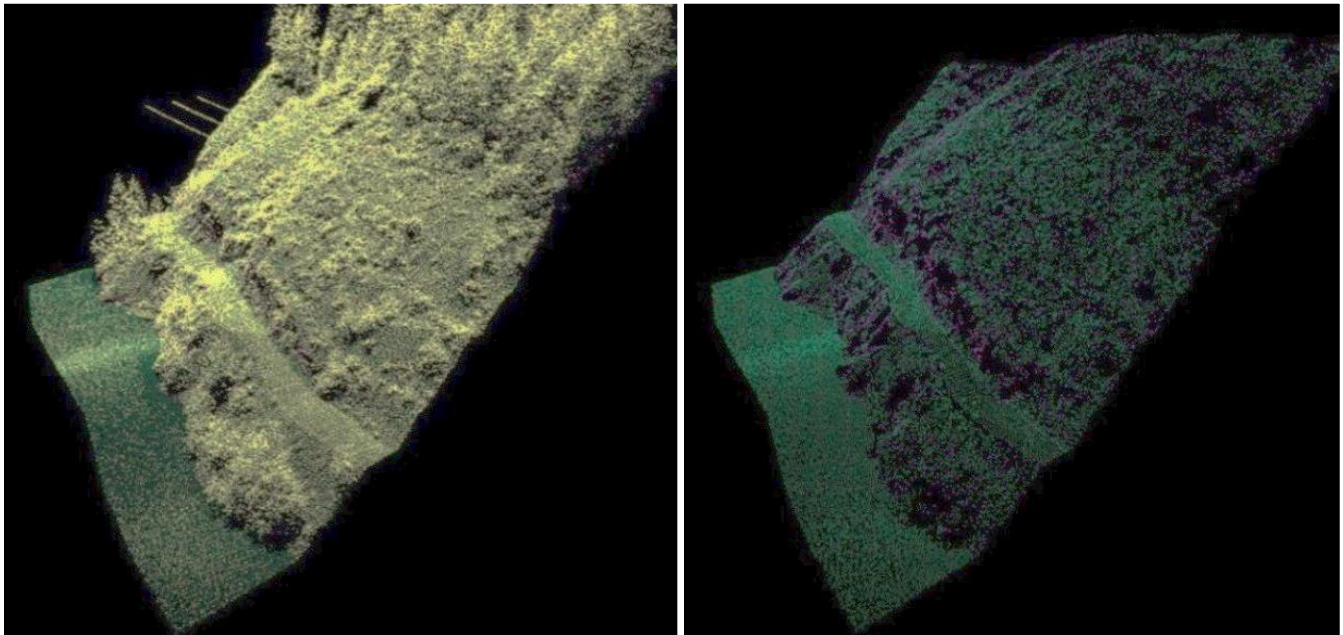
## LiDAR and LiDAR-Derived Data Files

Several LiDAR-related file types were associated with each 1x1-km tile (Figure 1).

**LAS (.las) file** — a standard data structure for storing point clouds along with many parameters such as classification and intensity. By connecting ground points into a triangular irregular network (TIN), the result is a DTM that can inform an analysis or a design. The delivered point clouds were classified either as “ground” or “unclassified”. The 107 .las files together comprised 31 GB, or 13 GB when compressed into .zip files (which is how the contractor provided the data).

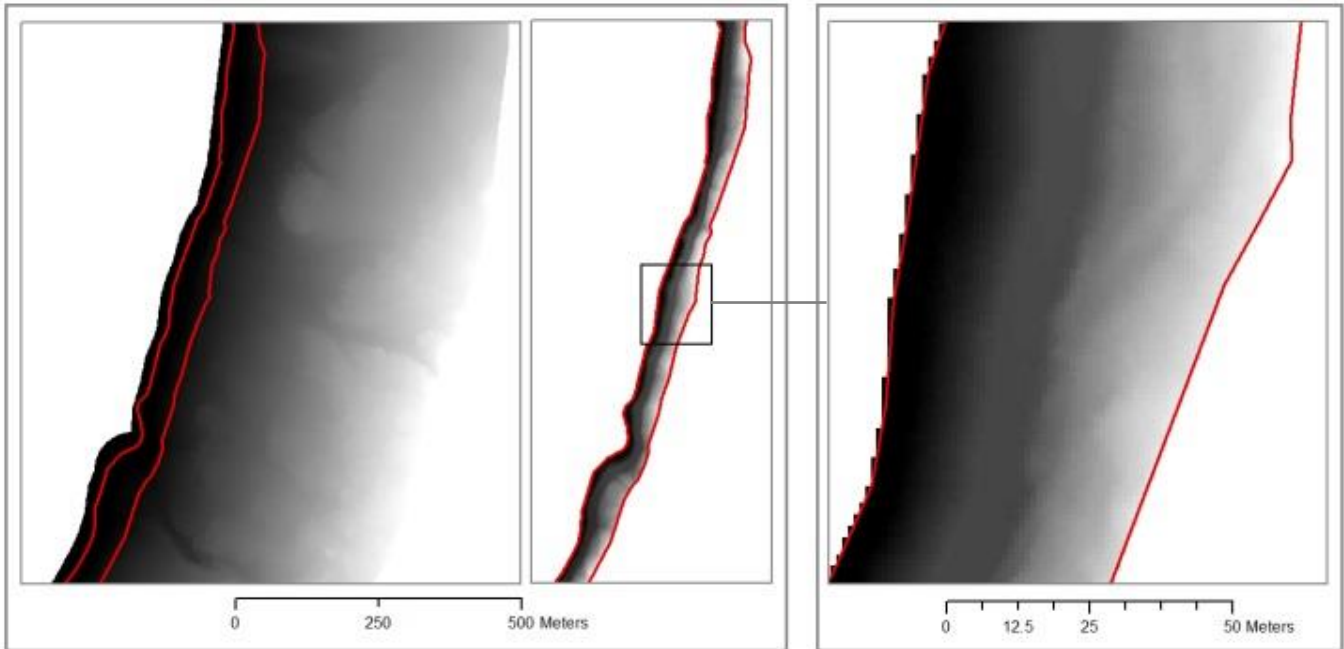
**Text (.xyz) file** — a text file that listed the coordinates of a subset of ground points called the model key points (MKPs). These same points resided in the .las file but were not classified as MKPs in the LiDAR data. MKPs can support the production of a simplified DTM that uses filtering algorithms to reduce the number of .las ground points without erasing the MKP points, or MKPs can be used alone to produce a simple DTM. The .xyz files together comprised 300 MB.

Figure 2 presents two 3D images that show how LiDAR represents a section of resource road.



**Figure 2: Two close-up 3D views of the same area along the In-SHUCK-ch FSR. Left: all LiDAR points, most of which are unclassified (yellow), are showing. Right: the unclassified points are removed, leaving those classified as ground points (green) and MKP points (purple), which form the subset of the ground points delivered as .xyz files**

**Raster (.img) file** — that was created by interpolating the .las ground points into a continuous 1x1-m pixel surface. Extraneous parts of the interpolated pixel surface can be clipped, and the file can be limited to the extent of the road corridor created (Figure 3). The .img format is native to IDRISI (remote-sensing software) and boasts read-write efficiencies due to its internal data structure. Some conventions refer to a raster-based ground model as a digital elevation model (DEM), as opposed to a DTM that is created from a TIN. Together, all the delivered .img files comprised 150 MB.



**Figure 3: DEM image files. Left: a DEM .img tile with the road corridor boundary marked in red. Middle: the same DEM clipped by the road corridor area and re-adjusted for colour scale. Right: a close-up of the clipped DEM.**

## Imagery Data Files

Associated with each tile were two main files containing collected imagery that had been ortho-rectified during post-processing and delivered with a resolution of 10 cm.

**Tagged image (.tiff) file** — a common raster format that features lossless compression, i.e., no information is lost during file compression (Figure 4, left). When the file has a geographic component, it is referred to as a GeoTIFF. In this form, it has an accompanying, very small, plain text file (.tfw) that describes its location. Together, the delivered GeoTIFFs comprised 30 GB, or 9.5 GB in .zip format (which is how the contractor provided the files).

**Compressed image (.ecw) file** — a common raster format that was originally developed for ERDAS (remote-sensing software). It is not entirely lossless, although any loss is very difficult to identify (Figure 4, right). Receiving orthorectified image files in .ecw format is advantageous for saving disk space; all the .ecw tiles for this project comprised only 600 MB.



**Figure 4: A comparison of two images obtained from different files, viewed in ArcGIS (ArcMap) software. Left: 10-cm resolution .tiff. Right: 10-cm resolution .ecw file. The slight differences in color are likely due to different default histogram settings used in ArcGIS software to view these images.**

## **Accuracy of the LiDAR and LiDAR-Derived Datasets**

In order to deliver the LiDAR and orthophoto datasets within FLNRO's accuracy specifications, the contractor had to successfully complete several tasks, such as calibrating the remote-sensing hardware, choosing a time to fly that would allow for maximum satellite reception and good weather, and making internal corrections to the data by running proprietary and custom software procedures.

While all of these topics are important, this report focuses to how ground-based Global Navigation Satellite System (GNSS) receivers played a part in georeferencing all data to ground coordinates, and in performing accuracy checks. The role of GNSS technology is central to the accuracy-reporting techniques of the datasets, and more generally, to any future surveys that will tie to the remotely sensed data via absolute coordinates of ground elevation, benchmarks, or control points.

## **Use of Control Points**

To georeference all the collected data to a specified coordinate system, the contractor tied into the Canadian Active Control System (CACS), a network of continuously operating and extremely accurate GNSS receivers (Figure 5, left). It was also possible to tie into other active control networks, such as the British Columbia Active Control System (Figure 5, right) or private networks, but the In-SHUCK-ch FSR happened to be located near two CACS stations: one in Whistler and the other in Chilliwack (Figure 5, left).

To make a tie-in possible, data were not only collected for the study area, but also over these two stations. When the two stations were identified in imagery, their locations were defined by the stations' published coordinates, which were then held fixed in the horizontal and vertical axis for both LiDAR and

imagery for all subsequent data post-processing. In other words, all collected data were georeferenced to these two 3D points.

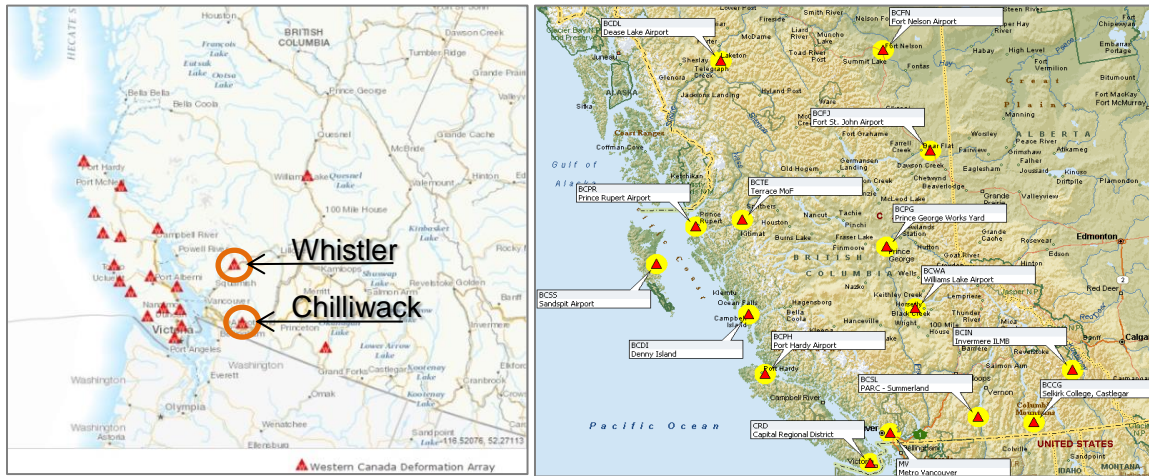


**Figure 5: Control points. Left: locations of all CACS stations in British Columbia. (Source: Natural Resources Canada website). The Whistler and Chilliwack stations were used for this study. Right: all operational British Columbia active control stations (source: GeoBC website).**

## Use of Checkpoints

To quantitatively validate the project’s absolute vertical and absolute horizontal accuracy requirements (the amount of allowable error), the contractor used four ground target locations on open and hard surfaces that were well distributed along the study corridor. At each of these four locations, two large pieces of white fabric—i.e., large enough to be visible in orthophotos—were laid out on the ground at a 90-degree angle (L-shape, Figure 6). Furthermore, a GNSS base station was set up over the target’s centre for at least 5 h in order to calculate a highly accurate 3D position. In the LiDAR contractor’s final report, these targets were referred to as “control points”; however, unlike the CACS station positions, these control points were not held fixed during the post-processing of LiDAR and imagery. So, to reinforce this distinction, this report refers to these as check points as opposed to control points.

The absolute vertical accuracy was checked by comparing the base stations’ calculated elevations to the corresponding 1x1-m cell value of the LiDAR-derived DEM raster, while the absolute horizontal accuracy was checked by visually measuring the distance between the base stations’ calculated coordinates and the centre of the target as seen in the 10-cm resolution orthophotos. The quantification of vertical accuracy was, therefore, independent of human judgement, whereas horizontal accuracy needed visual interpretation to identify the target’s centre on the orthophoto and in order to measure the horizontal distance to the GNSS base station-measured coordinates (Figure 6).

When checking a terrain model for accuracy, it is standard practice to reference LiDAR for the vertical component and orthophotos for the horizontal component (if both datasets are available and were collected by the same system). The reason that LiDAR is not used for horizontal checks or control is because it has less relative horizontal accuracy compared to imagery, i.e., it does not show ground targets with as much detail. When no images are available for horizontal control, it becomes necessary

to create some from LiDAR by interpolating between points, because LiDAR points cannot be guaranteed to hit particular targets. A common method for accomplishing this is to extract return intensity information for the points and create an intensity raster. The issue is that even with very dense aerial LiDAR, spacing between points will likely not support the creation of a raster that would come close to that of a high-resolution orthophoto (i.e., one with 10-cm resolution).

Vertical accuracy checks at the four checkpoints were reported using descriptive statistics (Table 1). The average difference between values derived from the GNSS base station (which are assumed to be the “true” elevations) and corresponding values from the LiDAR DEM was  $-1.80$  cm. The standard deviation (SD) was  $1.79$  cm, and the root means square error (RMSE) was  $2.38$  cm. Inferential statistics were not included in the report due to the small sample size. While the contractor could have included more checkpoints to support some inferential statistics, this would have increased the amount of field work and, therefore, the overall project cost.

Horizontal accuracy checks were also done at the same four checkpoints, but the results were not included in the LiDAR contractor’s final report; rather, they were summarized so as to conform to FLNRO’s accuracy requirements. The visual interpretation that is needed to accompany quantifying horizontal accuracy is illustrated in Figure 6. Since all the imagery was collected at the same time, using the same GNSS system as LiDAR, conclusions about the orthophoto horizontal accuracy also apply to the LiDAR dataset.



**Figure 6: Two 10-cm orthophotos showing the white fabric checkpoints, the base station coordinates (green dots), and black crosshairs, which illustrate the various interpretations of where the centres of the targets actually lie. The distance from the green dot to the crosshairs represents the absolute horizontal accuracy error of the orthophoto.**

**Table 1. Summary of vertical checkpoints**

Checkpoint	Elevation, by method		Difference in elevation Dz (m)
	LiDAR DEM (m)	GNSS <sup>a</sup> (m)	
1	36.070	36.109	0.039
2	166.630	166.629	-0.001
3	421.860	421.868	-0.008
4	233.060	233.086	-0.026

<sup>a</sup> Considered to be the “true” elevation.

<b>Avg. Dz (m)</b>	-0.018
<b>Max. Dz (m)</b>	-0.039
<b>Min. Dz (m)</b>	0.001
<b>Avg. Dz magnitude (m)</b>	0.018
<b>RMSE Dz (m)</b>	0.0238
<b>SD Dz (m)</b>	0.0179

## Absolute Accuracy Reporting

The LiDAR contractor’s report provided by the data-collection contractor included guarantees about absolute accuracy of the remotely sensed data that applied to flat, open, and hard surfaces, i.e., the type of terrain where the four checkpoints were located. The stated LiDAR absolute vertical accuracy was ≤0.2 m, and the stated orthophoto absolute horizontal accuracy was ≤0.3 m. These accuracy values were not derived using statistics from the four ground-truthed checkpoints, but rather, were based mostly on the contractor’s experience.

The reported accuracy statements refer to the RMSE statistic, which is a widely accepted method of quantifying the accuracy of position. In British Columbia, the official use of RMSE for reporting LiDAR accuracies is defined in a LiDAR specifications document (GeoBC 2014), which in turn references the American Society for Photogrammetry and Remote Sensing guidelines (ASPRS LiDAR Committee 2004).

Computing RMSE first requires a sample of ground-truth checkpoint observations that are at least three times more accurate than the model data. RMSE quantifies positional accuracy by summing individual squared differences between reference checkpoint measurements and corresponding locations in a model (e.g., DEM), then dividing by the number of differences, and finally, taking the square root:

$$RMSE = \sqrt{\frac{\sum_{i=1}^n (reference_i - model_i)^2}{n}} = \sqrt{\frac{\sum_{i=1}^n (error_i)^2}{n}}$$

The resulting RMSE statistic is a measure of the average total error in the sample data, meaning that it encompasses both random error (precision) and systematic error (bias). If the bias in the sample data is very low (close to zero), then the RMSE value will approximate the sample data’s SD which, by definition, quantifies just the sample data’s average random error:

$$SD = \sqrt{\frac{\sum_{i=1}^n (error_i - mean.error)^2}{n-1}}$$

The error term in the SD equation refers to the difference between the reference and model values (see preceding equation), and the mean error is the average of these errors. Furthermore, if the individual errors from the RMSE calculation follow a normal curve, this makes it possible to use the well-known Z-table probability distribution to report RMSE at certain confidence levels.

The guidelines of the American Society for Photogrammetry and Remote Sensing (ASPRS LiDAR Committee 2004) state that LiDAR vertical accuracy should be reported using RMSE at 95% confidence level, but the guidelines do not specify a horizontal accuracy reporting method.<sup>1</sup> The guidelines also state that the checkpoint measurements used to produce vertical RMSE statistics need to come from relatively flat, smooth, and open locations where a normal distribution of error is expected. Given that this approach uses RMSE along with confidence levels, the underlying assumptions include that the residuals have no bias and are normally distributed (Zandburgen 2008). In other conditions, such as under canopies or on slopes, the chances of RMSE containing bias and/or having a skewed distribution are greater. In these situations, using the Z-table to compute RMSE at a given confidence level would be inappropriate. Instead, the guidelines of the American Society for Photogrammetry and Remote Sensing (ASPRS LiDAR Committee 2004) suggest the percentile method may be used to report confidence levels.

While the LiDAR contractor reported that the absolute vertical accuracy was  $\leq 0.2$  m, and the orthophoto absolute horizontal accuracy was  $\leq 0.3$  m, the following would be a more detailed expression of this statement: the absolute vertical accuracy of the LiDAR dataset was  $\leq 0.2$  m RMSE at 95% confidence level, and the absolute horizontal accuracy of the orthophotos was  $\leq 0.3$  m RMSE at 68% confidence level.<sup>2</sup> Taking vertical accuracy as the example, the practical implication is: if a new ground-truthed elevation is obtained on similar terrain and is compared to the LiDAR model value, there is a 95% probability that the elevation difference found would be  $< 20$  cm. Also, using the LiDAR accuracy statement, it is possible to calculate that the RMSE value is 10.2 cm, which corresponds to a 68% confidence level (because  $1.96 * (\text{RMSE}) \leq 20$  cm, with the value 1.96 coming from the two-tailed 95% confidence level on the Z-table).<sup>3</sup> It is worth emphasizing that the RMSE statistic does not make inferences about RMSE for the data population (all possible measurable errors); using  $1.96 * (\text{RMSE})$  to describe sample residuals already presumes that no bias exists (Congalton and Green 2008).

For the In-SHUCK-ch project, the contractor used the four checkpoints to find an average difference (bias) in elevation of only  $-1.8$  cm (see Table 1), and this provided some evidence of no significant bias. The four checkpoints also had a reassuring RMSE value of 2.4 cm, which meant that if this RMSE value was truly representative of the entire population of errors, the vertical absolute accuracy of LiDAR would be 4.7 cm RMSE at a 95% confidence level. This evidence from the four checkpoints, along with experience, allowed the contractor to be comfortable in guaranteeing that, within the project's coverage area, the vertical absolute accuracy of LiDAR would be  $\leq 20$  cm RMSE at a 95% confidence level for

---

<sup>1</sup> New guidelines from the American Society for Photogrammetry and Remote Sensing (2014) recommend reporting horizontal accuracy using the RMSE at 95% confidence level statistic, as outlined by the U.S.A.'s National Standard for Spatial Data Accuracy (Federal Geographic Data Committee 1998).

<sup>2</sup> This was the horizontal accuracy reporting method specified by FLNRO to the LiDAR contractor.

<sup>3</sup> When reporting horizontal accuracy using the American Society for Photogrammetry and Remote Sensing's draft guidelines (ASPRS LiDAR Committee 2004, see footnote 1 above), note that the x and y axes are treated separately; and, similar but not identical statistical formulas are used to calculate vertical accuracy.

any flat, open, hard surfaces. The use of only four checkpoints was not in compliance with the guidelines (ASPRS LiDAR Committee 2004) which suggest at least 20 checkpoints be used; however, having less checkpoints reduced costs.

## Relative Accuracy Reporting

Only the LiDAR dataset reported a relative accuracy and it was  $\leq 0.1$  m. In this instance, relative accuracy refers to the internal accuracy between LiDAR strips flown from different flight lines. It represents the allowed tolerance for adjusting the elevation of features to achieve agreement of elevation values of the same features on overlapping LiDAR flight strips. These elevation discrepancies were corrected during post-processing, presumably with proprietary methods.

The reported  $\leq 0.1$  m accuracy presumably refers to root mean square difference (RMSD) at 68% confidence level, which would follow British Columbia's LiDAR specification guidelines (GeoBC 2014).<sup>4</sup>

## FIELD METHODS

In order to validate the accuracy of the LiDAR dataset for the different types of terrain that occurred along the road it was necessary acquire new GNSS points.

The new GNSS points were obtained by FPIinnovations using two approaches: (1) collecting GNSS points for existing FSR conventional survey markers to allow for direct comparison of the conventional survey DTM to the LiDAR DTM, and (2) collecting GNSS points at selected small areas along the FSR to acquire small samples of ground-truthed DTM relative to the DTMs derived from the LiDAR and conventional surveys.

Unlike the checkpoints collected by the contractor, both of these approaches collected checkpoints after LiDAR and imagery had been flown. The new checkpoints would therefore be useful only for vertical accuracy checks because they would not be distinguishable in orthophotos.

## Constraints in Using GNSS to Check LiDAR Accuracy

When many new points are being collected, and high accuracy is required, a common approach is to pair a GNSS base station with a mobile GNSS rover unit to produce real-time-kinematic (RTK) satellite navigation. The mobile GNSS rover unit is used to collect new points while in communication with the stationary base station, which collects data from satellites to precisely define its location. One constraint

---

<sup>4</sup> When discussing relative accuracy the term RMSD is used in place of RMSE, because using the word “error” implies a difference between an estimate and a true, known value. In the case of a difference between two LiDAR datasets, neither is the true value, i.e., neither has considerably greater absolute accuracy—so it is simply referred to as a difference rather than an error (American Society for Photogrammetry and Remote Sensing 2014). Confusingly, the acronym RMSD is sometimes used interchangeably with RMSE; but, in this case the acronym RMSD stands for root mean square deviation.

Another confusing point is that, when discussing LiDAR, the term “relative accuracy” may be used to refer to any point-to-point measurement. In this usage, relative accuracy depends on the density of the point cloud. For example, when measuring the width of a bridge using LiDAR, there is only a probability that the two points used actually hit exactly the bridge edges. As the density of a point cloud increases, this effect becomes more negligible.

to this method is that the rover requires a link with the base station and its own lock on overhead satellites in order to collect an accurate location for a new point (relative to the base station). After field work is complete, the rover-collected coordinates can be corrected using the observations at the base station.

Another constraint is that the maximum distance between the base station and rover depends on the landscape (i.e., mountains can block signals) and on the GNSS specifications of the system. Generally, the range of the rover is at least a few kilometers but this can be increased by including a radio amplifier in the RTK system.

After the post-processing of all collected data is complete, typically the accuracy for the location of the base station is about 1.5 to 4 cm vertically, and 1 to 2 cm horizontally (at a 95% confidence level). The accuracy of points collected by the rover further depends on the distance from the base station. A typical RTK system will provide 2 ppm accuracy for rover points in both the vertical and horizontal direction—in other words, a 2-cm vertical and horizontal error for every 10 km. Given that the In-SHUCK-ch FSR LiDAR has reported vertical accuracy of  $\leq 20$  cm (@95% confidence), maintaining an accuracy that is three times better than LiDAR would require that points collected by rover have a vertical accuracy of  $\leq 6.66$  cm (@ 95% confidence). Assuming that the base station component of this error is a relatively poor 4 cm, this leaves  $\leq 2.66$  cm of error available to be accrued by the rover component. The rover, therefore, can be up to about 13.3 km away and still maintain the required accuracy. More optimistically, if the base station accuracy is 1.5 cm, the allowable distance of the rover increases to approximately 25.8 km—assuming that rover-to-base-station reception is still possible.

## Field Work

FPInnovations had several meetings with FLNRO and consultants familiar with the In-SHUCK-ch FSR to identify and select suitable areas of the road for studying the limitations of LiDAR. The consensus was to focus on three 2-km sections of road that had previously been surveyed using conventional ground methods.

The start points of these three road sections were near KM 6, KM 20, and KM 44 of the road. These road surveys, whose original purpose was to inform road re-alignment, were several years old and encompassed a variety of terrain and vegetation types, and included survey sections that used total station as well as hand survey methods.

The established plan for field work at these three road sections included two field trips. The first trip would georeference the conventional surveys and then, back in the office, the resulting ground-survey DTM would be aligned and compared to the LiDAR DTM. The second field trip would use this comparison to identify areas of discrepancy so that new data points could be obtained and act as a ground truth to the datasets obtained from both the conventional surveys and the LiDAR survey, i.e., in order to compare the resulting earthworks calculations.

### *First Field Visit*

On February 3rd and 4th, 2014, FPInnovations researchers travelled from Vancouver to the In-SHUCK-ch FSR in the Chilliwack Forest District, with Onsite Engineering Ltd., a consulting company with

surveying expertise. The purpose of this field visit was to find and georeference as many old ground survey markers as possible at each of the three road sections that had been identified for study.

The RTK system, including an amplifier, was supplied by Onsite Engineering. On the first day, the base station was set up in an open area near KM 23, and the amplifier was placed about 10 m away (Figure 7). While the GNSS receiver at the base station collected data for over a 5 h period, the rover GNSS was used for georeferencing along with a total station, which was needed primarily to tie to benchmarks on vertical surfaces (trees). This base station location allowed for the georeferencing of ground survey benchmarks in the surveys near KM 20 and KM 44.



**Figure 7: Georeferencing field equipment. Bottom Left: the RTK system set up near KM 23. On the left is the base station positioned over the benchmark, and the amplifier is in the foreground. Upper Left: a close-up of the benchmark. Right: Onsite Engineering field staff using the rover to georeference a survey stake.**

Along the KM 20 section, the rover performed well except for two benchmarks where the rover was unable to acquire a satellite lock—likely due to the abundance of canopy overhead. A workaround could have involved using a total station to traverse to these benchmarks from nearby georeferenced benchmarks; however, this would have been time consuming. Therefore, it was decided to re-attempt a satellite lock with the rover on the following day.

Along the KM 44 section the rover received signals from the base station at all times. The base station was no more than 23 km away and had never had any satellite reception issues. A 23-km-roaming distance was deemed to meet the study's accuracy requirements because elevations measured from the same base station location on a previous occasion had a vertical accuracy of 1.5 cm. This left 5 cm of error that the rover could have, which theoretically would happen at a roaming distance of 25 km. Several old survey markers were found along the KM 44 section and these took less time than anticipated to georeference. With the extra time available, additional nearby survey markers were georeferenced on the adjacent KM 42 km section, which was 2 km long.

### **Second Field Visit**

On February 4th, the base station was re-established near KM 23 in order to georeference the remaining benchmark locations along the KM 20 survey. Since the base station location had now been occupied for more than 5 h on two separate occasions (the location had been used once previously for a different purpose), it needed to be set up for only a short time to reference the remaining benchmarks with the rover. The rover was able to obtain the benchmark locations on this second attempt, likely due to more favourable satellite constellations.

The base station and amplifier were then moved to near KM 6 (adjacent to the beginning point of the ground-based survey). More survey markers were found and georeferenced along this 2-km-long survey than for other two surveys (Figure 8), and no signal reception issues were encountered.



**Figure 8: Two examples of the types of survey markers encountered on the In-SHUCK-ch FSR. Left: a property survey (intersection point) marker. Right: a wooden survey stake.**

### **Processing the Data from the First Field Visit**

Base station observation data were post-processed using Natural Resource Canada's free Precise Point Positioning (PPP) automated service, and were exported in the NAD83 (CSRS) coordinate system. The final errors of the base station were <1.5 cm in the vertical direction. This post-processing also shifted all of the rover-collected points relative to the new, refined base-station position.

An alternative approach to the PPP service would have been to use a private service (and associated software), which likely would have produced an even higher accuracy through the availability of more active base stations and/or the ability to support more complex field methods. This was the approach that the remote-sensing contractor took for the post-processing of base station observation data at the four checkpoints distributed over the project area, but the 95% confidence level accuracy values for these checkpoints were not included in the contractor's final report.

Onsite Engineering imported all of the rover-collected points into RoadEng road design software, and then proceeded to use them to align (georeference) the conventional as-built ground surveys. The alignment methodology used two georeferenced points: one was held fixed directly over the associated point in the ground survey, and then the ground-survey was rotated so that overall error was minimized. No adjustments were made in the vertical direction. For each section, this process was repeated with different combinations of points until the best overall fit was found, with errors being assessed both through measurement and visual inspection.

Georeferencing of the survey markers within the ground-based surveys revealed several issues that were suspected to originate from the pre-existing ground-survey methods, but horizontal accuracy of GNSS rover and the LiDAR data may also have had an effect. Along the KM 6 survey, even though there were a large number of georeferenced points, it turned out that most of these were not referenced in the as-built survey, and using any combination of the remaining survey points always resulted in relatively large horizontal errors; the rotated point would at times be up to several meters from its expected position. The KM 20 survey aligned very well except for the beginning of the survey where rover reception issues were encountered and, therefore, the first 500 m of this survey were excluded from the study. Alignment along the KM 42 survey (the additional section that was surveyed) was very poor except for the last 500 m that were adjacent to the start of the KM 44 survey. The KM 44 survey alignment was good but only when the survey was split into two parts and individually aligned.

The result was that data for only two sections of the road were usable, and these two sections are the focus of the remainder of this report. The sections are here referred to as Road Section A, which was started at KM 20.47 (referred to here as KM 20) and was 1.5 km long, and Road Section B which started at KM 43.63 (referred to here as KM 44) and was 2.3 km long.

The conventional survey at Road Section A used a total station, while Road Section B likely used a total station for the centreline and some form of handheld gear (laser or compass) for side shots (the exact survey method was undocumented). Together, these two sections did manage to comprise all the types of terrain and cover the intended study area, including steep slopes, cliffs, and flat areas; and each of these terrain types included some canopy and non-canopy areas.

Figure 9 shows a close-up of the existing as-built survey of points and breaklines that were georeferenced at Road Sections A and B.

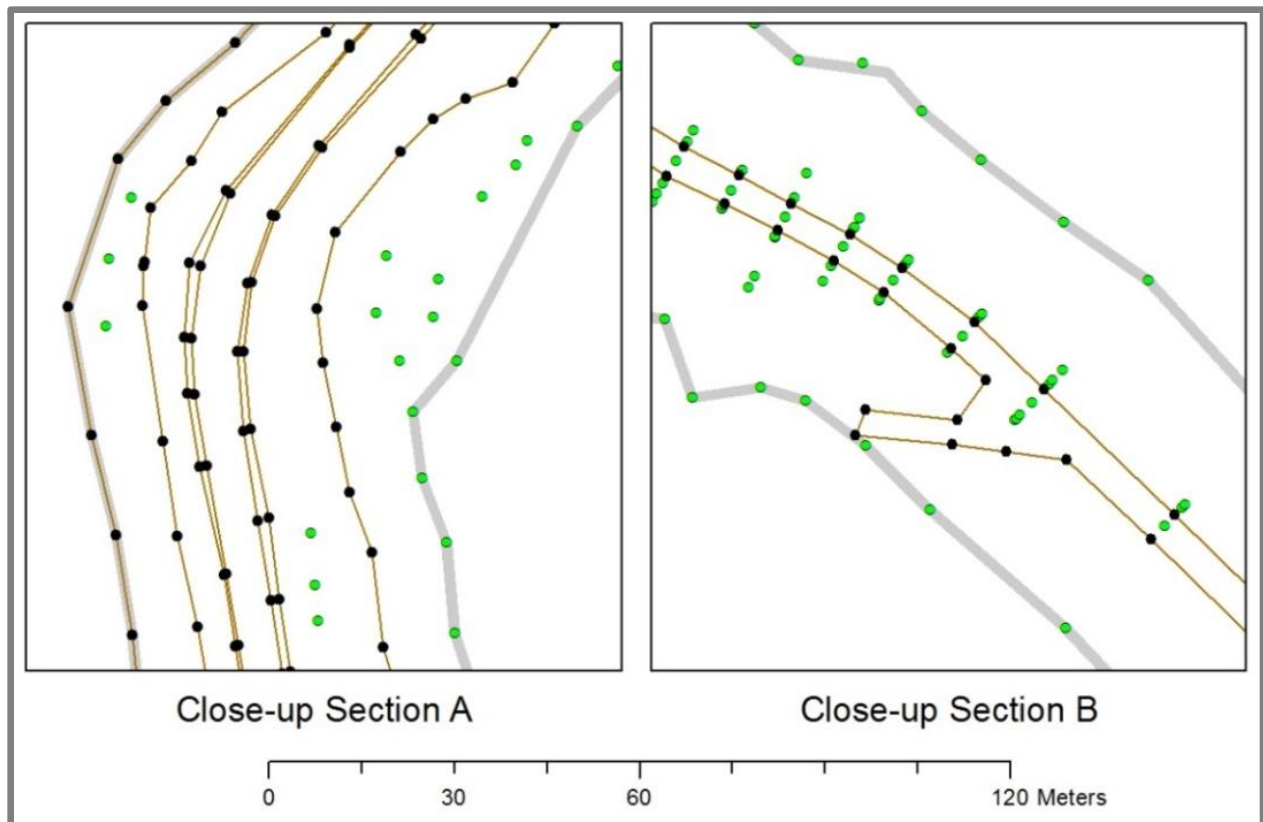


**Figure 9: Close-ups of conventional surveys at Road Section A and Road Section B. The black dots represent elevation points that are part of breaklines, shown in brown. Breaklines are straight lines between two points that can be used to force creation of the edge of a triangle during a triangulation that makes a TIN. The green dots represent elevation points not associated with breaklines, and the grey lines delineate the boundary of the survey. The sets of elevation points in a perpendicular line to the road in Road Section B are indicative of handheld side shots.**

### **Second Field Visit**

On March 31st to April 2nd, 2014, Onsite Engineering Ltd. made a second field visit to the In-SHUCK-ch FSR. The purpose was to collect dense sets of points at three subsections within the 1.5-km-long Road Section A, and at three subsections within the 2.3 km-long Road Section B in order to have some data that could be ground truth for earthworks calculations. These six short subsections (~25 m long) were considered good locations because they had a variety of canopy and slope conditions, and included some discrepancies between the LiDAR and conventional survey methods (Table 2).

**Table 2: Road subsections where detailed total station surveys were completed**

Road Section and Subsection	Location	Length (m)	Description
Road Section A <sup>a</sup>			
Subsection A1	KM 21+062 to 21+130	68	Steep slope. Canopy over road, canopy on downhill side. Canopy and bare earth on uphill side.
Subsection A2	KM 21+585 to 21+608	23	Steep slope. Canopy on downhill side. Shrubs and bare earth on uphill side.
Subsection A3	KM 21+740 to 21+762	22	Steep slope. Canopy on downhill and uphill sides. Stream crossing.
Road Section B <sup>b</sup>			
Subsection B1	KM 43+945 to 44+972	27	Flat area. Canopy on one side of road. Bare earth and shrubs on the other side.
Subsection B2	KM 45+206 to 45+233	27	Steep slope. Canopy, shrubs, and open sky on both sides. Stream crossing.
Subsection B3	KM 45+735 to 45+763	28	Very steep (cliff on uphill side). Canopy and open sky on both sides.

<sup>a</sup> Total station.

<sup>b</sup> Total station for the centreline plus side shots based on (undocumented) hand-survey methods.

Onsite Engineering used a total station to collect points, and georeferenced these points using the same RTK system as in the first field visit. No satellite reception issues were encountered.

Figure 10 illustrates the density of this detailed total station survey compared to the previously completed conventional total station survey and the LiDAR ground points.

### *Processing of the Data from the Second Field Visit*

Post-processing the survey data simply involved uploading the base station observations to the PPP service, just as was done with data from the field visit.

Figure 10 is an example of detailed total station data collected at Road Subsection A3 in relation to the previously completed total station survey (upper right), and it compares the density of the ground-based survey.

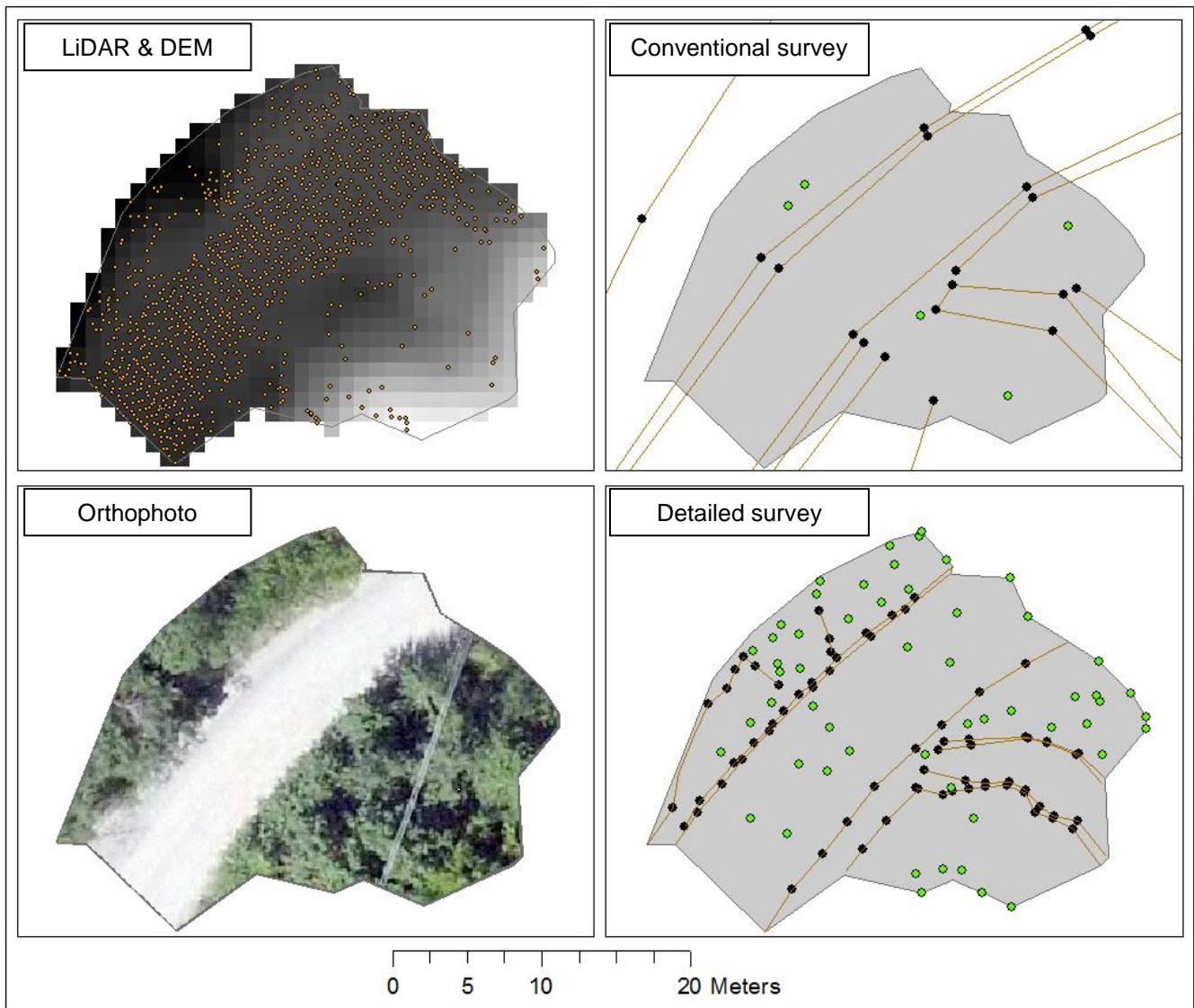
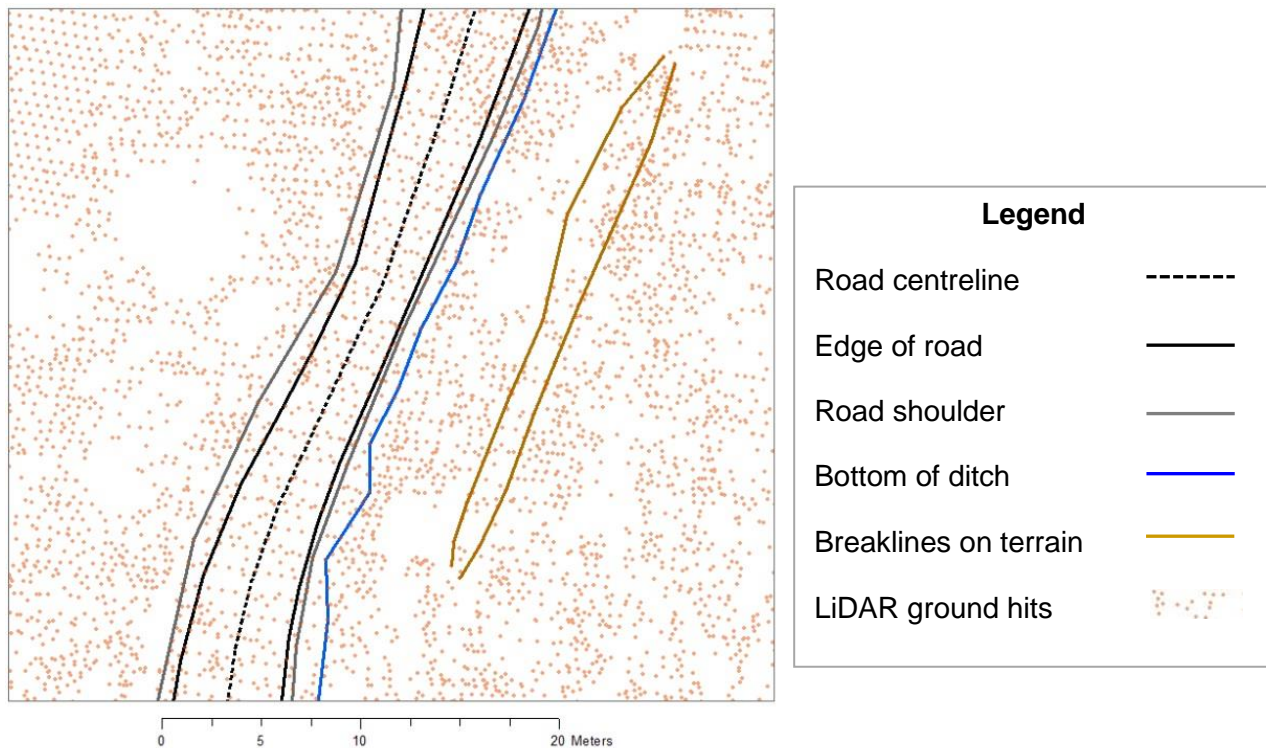


Figure 10: Four representations of Road Subsection A3. **Bottom Right:** the detailed total station survey. **Upper Right:** the conventional survey that used a total station. In these two surveys, the green dots represent elevation points not associated with breaklines, while the black lines are points that define breaklines, which are shown in brown. **Upper Left:** the LiDAR ground hits along with the related DEM raster in the background. The LiDAR ground points are shown in orange. The 1x1-m DEM raster was derived by creating a TIN from LiDAR points and then rasterizing the result. The darker pixels are lower compared to the white areas, and the elevation ranges from 203 to 213 m. The relatively few number of LiDAR ground points in the higher elevation area is caused by canopy that can be seen in the orthophoto. **Bottom Left:** the 10-cm orthophoto.

## Post-Survey Breaklines

While FPIinnovations was preparing and analyzing data from the second field visit, FLNRO asked the remote-sensing contractor to deliver post-survey breaklines derived from LiDAR and imagery for Road Section A. This work was intended to inform a future comparison of the accuracy of post-survey breaklines to that of conventionally derived ground survey breaklines; however, the contractor delivered the data with a quick turnaround and so the data were also available for this study.

Figure 11 shows a close-up of the post-survey breaklines that were delivered as a .dwg file. Using these breaklines together with the LiDAR to produce a TIN and/or DEM points produces a more accurate result compared to using just the LiDAR points.



**Figure 11: Close-up view of breaklines in Road Section A.**

## EVALUATION OF ACCURACY

Data from all the completed field work allowed for the comparison of DTMs derived from the LiDAR survey to those derived from conventional surveys in terms of vertical accuracy and volumetric earthworks calculations. The smaller-scale data at Road Sections A and B supported accuracy evaluation at distinct points, and the larger-scale data at the six subsections acted as the ground-truthed terrain for earthworks calculations.

## Data Preparation

Comparing the accuracy of the LiDAR survey to that of conventional ground surveys is not a straightforward task. For LiDAR ground points, any differences in accuracy mainly depend on the surrounding terrain features, while for ground-surveyed points, accuracy instead relates to the length of traverse (and potential blunders). Furthermore, for both types of surveys, when points are interpolated to a DTM surface, the potential for inaccuracy to occur increases with distance from the survey points. With LiDAR, interpolation distances are generally larger under canopy conditions due to sparser ground point spacing, while in ground surveys, interpolation distances depend on the judgement of the surveyor, the ease of access to terrain, and the time allotted for surveying.

FPIinnovations prepared the data for statistical analysis with the following software:

- ArcGIS for organizing files and for 2D cartography.
- Global Mapper for classifying hydro lines (so they would not interfere in the creation of canopy height rasters).
- FME for all data cleaning, transformations, deriving new datasets from LiDAR, format conversions, and 3D visualization.
- Excel to summarize results.

### *Selecting a Reference Terrain Model*

The LiDAR survey was selected as the reference (i.e., true measurement, see the equation in the section above called Absolute Accuracy Reporting) because the conventional survey had no known accuracy outside of the points that were georeferenced. Choosing the conventional survey as the reference instead would only have impacted the signage of statistics (i.e., a positive bias result would be negative). Resulting errors were assumed to originate from the LiDAR data.

### *Filtering Points by Horizontal Proximity*

Many conventional survey points in Road Section A were up to 1 m or so away from the closest LiDAR point. Furthermore, in Road Section B, distances were greater because the conventional survey was sparser (see Figure 9).

While it would be possible to obtain an error at each conventional survey point by subtracting it from an interpolated value derived from the LiDAR DEM, the results from this type of analysis would measure the accuracy of the DEM interpolation method, which was not the aim of the study. For this reason, the only errors included in our statistical analysis were those where a LiDAR point was within 0.5 m of a conventional survey point. A smaller distance would have been more ideal because it could reduce vertical errors due to a difference in horizontal position, but using a smaller distance resulted in an error sample size that was too small. In Road Section B, points also needed to be closer than 7 m from the surveyed road centreline in order to remove hand-surveyed points that most likely had much lower accuracy than the LiDAR points (7 m was judged to be the approximate limit of where points began to have a vertical accuracy of <15 cm).

Once points in Road Section A and Road Section B were filtered using the distance constraint, errors were recorded by subtracting the conventional survey point value from the LiDAR DEM raster cell

value. The points collected at the six subsections were not used to assess vertical accuracy because they did not include enough conventional points that corresponded to a LiDAR point within 0.5 m.

### *Making Slope and Canopy Raster Layers*

The next data-preparation step was the creation of slope and canopy information layers, because the vertical accuracy of LiDAR needed to be evaluated under terrain conditions that included: (1) flat and open, (2) flat with canopy, (3) steep and open, and (4) steep with canopy.

Both slope and canopy layers were prepared as raster layers with the same extent and cell size as the LiDAR-derived DEM. Generally, creating a slope layer is a task that any GIS can accomplish because it requires only a DEM for input; deriving a canopy-height DEM is more involved because it requires the elevation DEM and the above-ground LiDAR points, and can include various post-processing techniques to remove artifacts.

Figure 12 shows a sample of the DEM, the slope raster, and the canopy height raster for Road Section A.

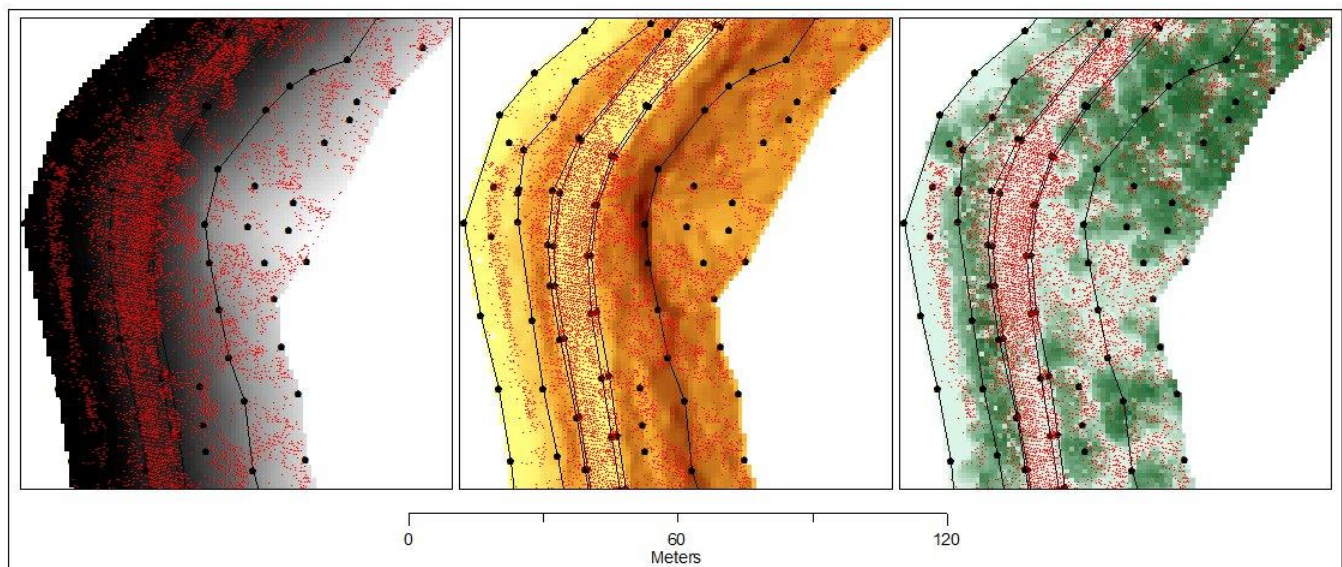


**Figure 12: Close-up of Road Section A. Left: Digital Elevation Model on which black represents the lowest elevations and white the highest elevations. Middle: Slope Model. Yellow is the gentlest slope and brown is the steepest slope. Right: Canopy Model. Light green areas are open while dark green are closed canopy of tall trees. Red dots are LiDAR ground points, and black dots and lines are from the conventional total station survey.**

## **Differences Between LiDAR and Ground-Survey Terrain Models**

To evaluate the accuracy statement that LiDAR will be  $\leq 20$  cm RMSE at a 95% confidence level for any flat, open, hard surfaces, it was assumed that flat terrain had a  $\leq 3$ -degree grade, and that “everywhere” was a hard surface. This resulted in a sample of 32 errors in Road Section A, and 48 errors in Road Section B. The RMSE at 95% confidence level was 18 cm for Road Section A, and 11 cm for Road

Section B. Road Section A had a significant bias of +6.4 cm, and Road Section B also had a significant bias of -2.4 cm (Figure 13). Table 3 also summarizes these results.

Using this same slope condition of 3 degrees to evaluate flat-with-canopy conditions produced only 14 errors in Road Section A and 8 errors in Road Section B; therefore, the slope constraint was relaxed to <6 degrees. While this still did not produce a large enough sample size in Road Section B, in Road Section A, 32 errors resulted that had a 95% percentile error of 34 cm, and a significant bias of +16 cm (Figure 14). Table 4 also summarizes these results.

In order to have a consistent slope limit that produced large enough sample sizes in both open sky and canopy conditions, the accuracy for flat, open sky conditions in Road Section A and B was re-calculated to include all slope values  $\leq 6$  degrees (Figure 15). In Road Section A this produced 85 errors with an RMSE of 23 cm at a 95% confidence level and a significant bias of +7.8 cm, and in Road Section B an RMSE of 16 cm at a 95% confidence level and a significant bias of +2.9 cm. Table 4 also summarizes these results.

When calculating the accuracy for points in steep areas, for both the open sky and canopy conditions, steep was defined as areas with  $\geq 25$  degrees slope. This produced both kinds of errors in Road Section A, but none in Road Section B because most points on steep slope were discarded because they were more than 7 m away from the road centreline. In Road Section A, there were 26 errors in steep, open sky conditions with a 49 cm error at the 95<sup>th</sup> percentile and insignificant bias of 7.5 cm, and 128 samples of errors in steep and canopied conditions, which had an accuracy of 61 cm at the 95% percentile, and a significant -29 cm bias (Figure 16). Table 5 also summarizes these results.

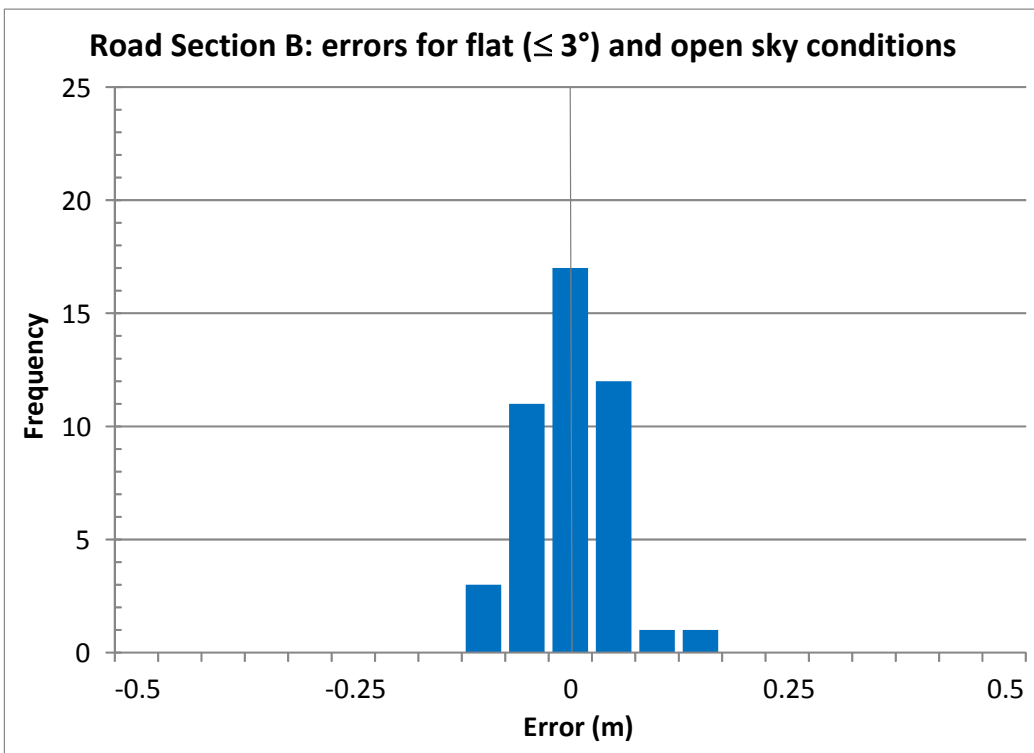
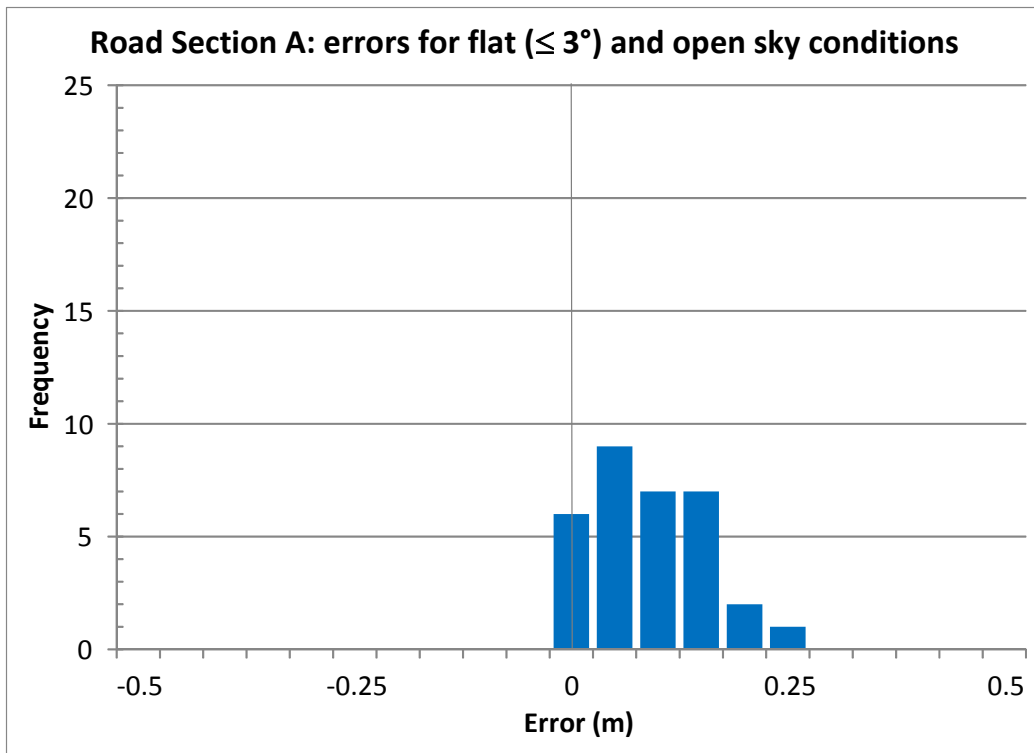


**Figure 13: LiDAR error distribution in Road Section A and B for flat terrain with open sky, where flat is defined as  $\leq 3$  degrees slope.**

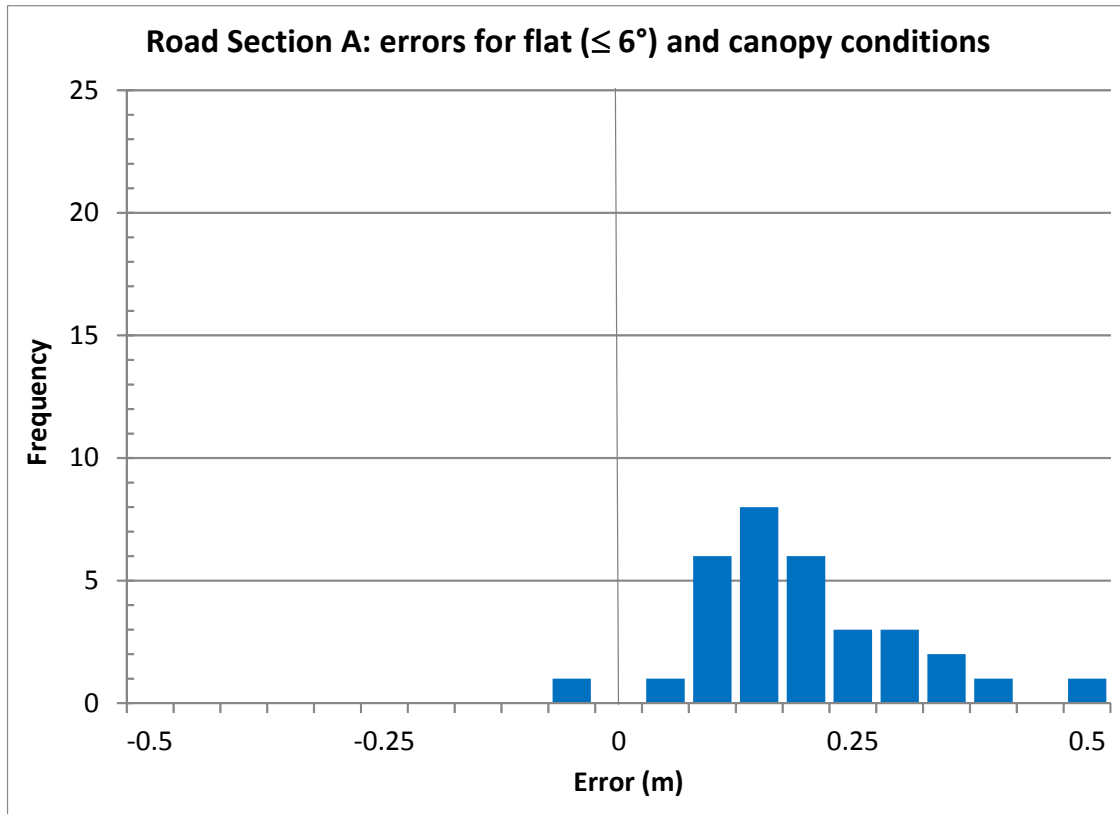
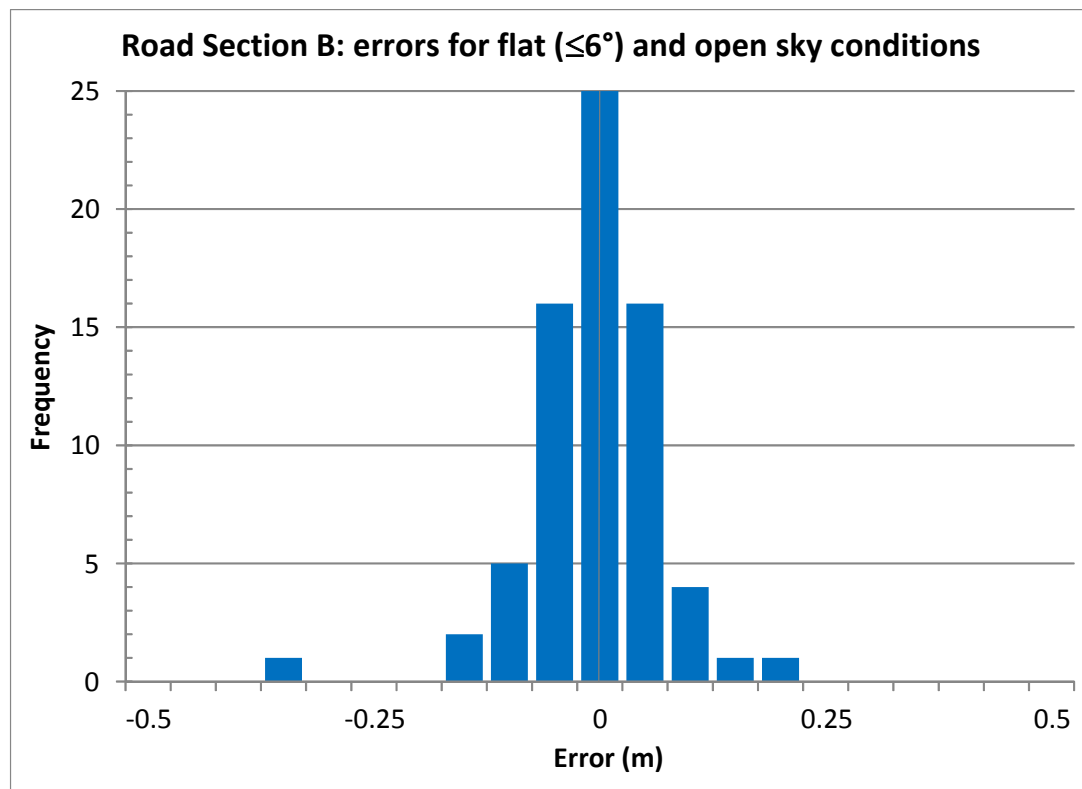
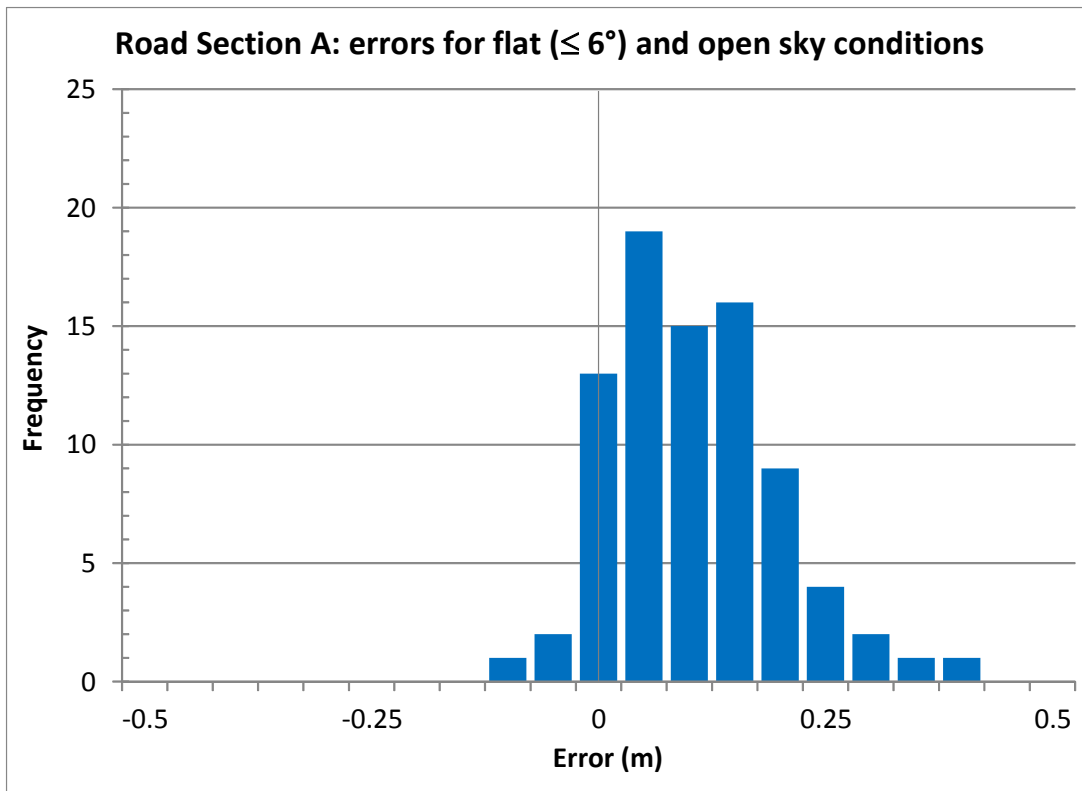


Figure 14: LiDAR error distribution in Road Section A for flat terrain with canopy, where flat is defined as  $\leq 6$  degrees slope.



**Figure 15: LiDAR error distribution in Road Section A and B for flat terrain with open sky, where flat is defined as  $\leq 6$  degrees slope.**

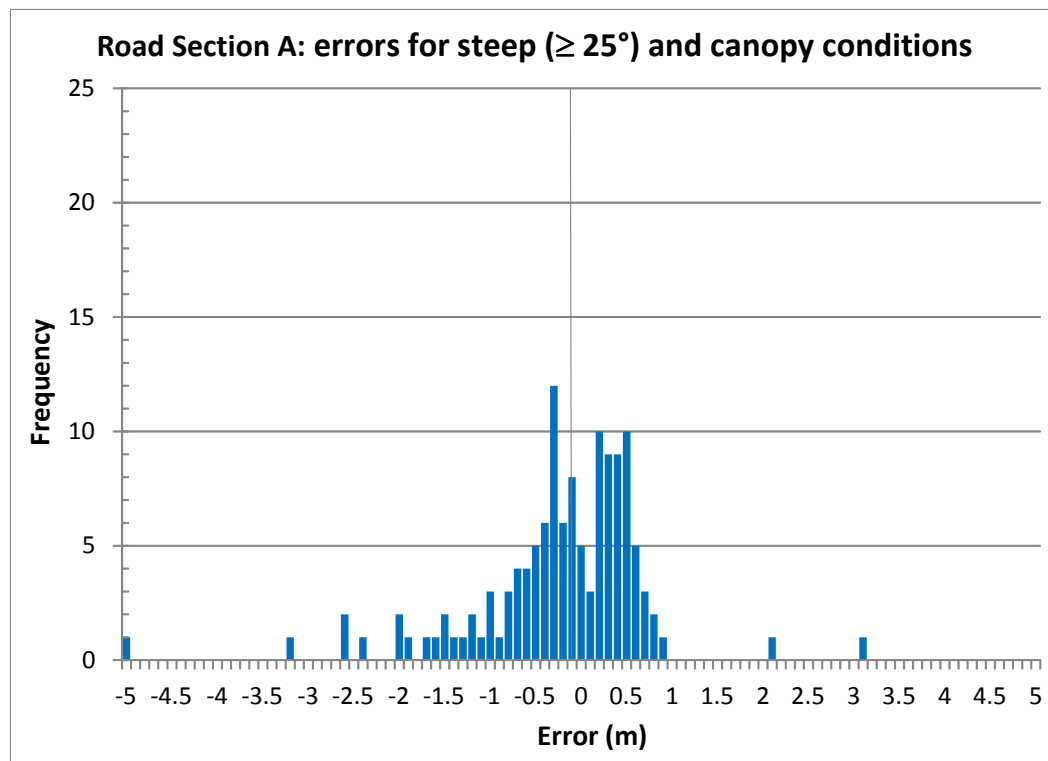
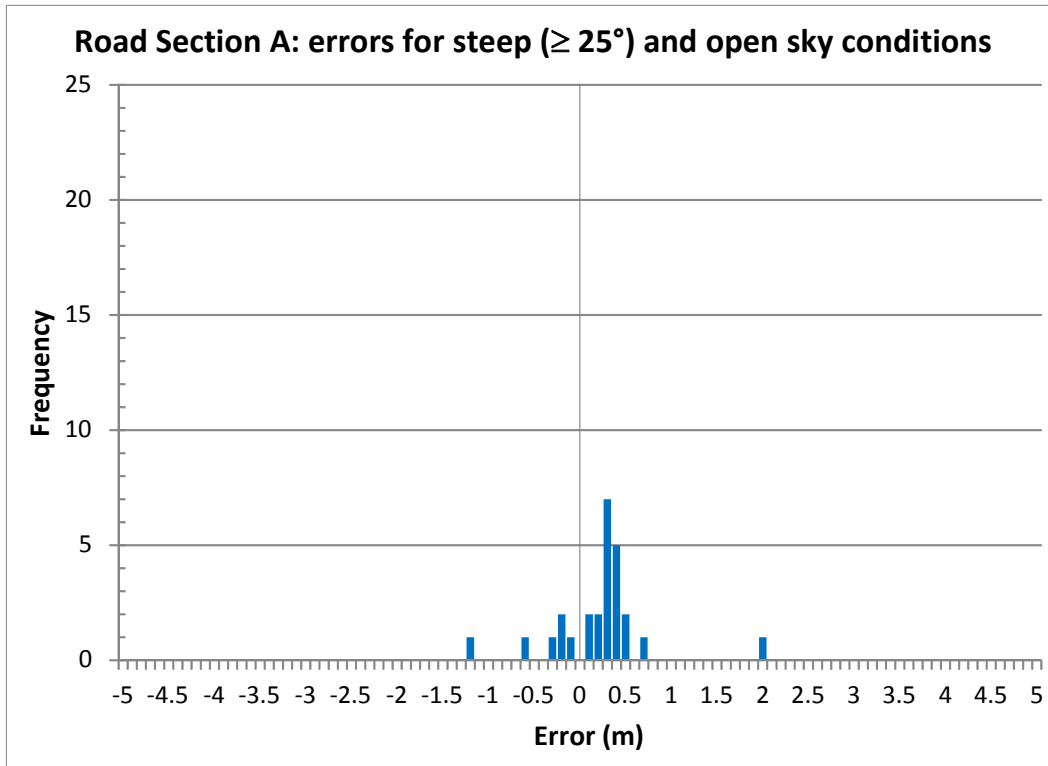


Figure 16: : LiDAR error distribution in Road Section for steep terrain with open sky conditions (top) and steep terrain with canopy (bottom), where steep is defined as  $>25$  degrees slope.

## Summary and Discussion of Vertical Accuracy Results

Table 3, Table 4, and Table 5 summarize the histograms in Figure 13, Figure 14, Figure 15, and Figure 16, respectively. Table 3 summarizes the accuracy results in flat and open sky conditions from which allows for the testing of the LiDAR vendor's accuracy claims in Road Sections A and B. Table 4 presents the same results for Road Sections A and B but uses the less stringent slope definition of 6 degrees. Table 5 presents errors in Road Section A for terrain conditions that are flat with canopy, steep with open sky, and steep with canopy.

**Table 3: Accuracy associated with LiDAR data, for flat terrain with open sky, where flat is defined as  $\leq 3\%$  slope**

Road Section	Conditions	Error (cm)	Statistic	Error sample (no.)	Bias <sup>a</sup> (cm)
A	Flat ( $\leq 3$ degrees) and Open	18	RMSE*(1.96)	32	<b>+6.4</b>
B	Flat ( $\leq 3$ degrees) and Open	11	RMSE*(1.96)	48	<b>-2.4</b>

<sup>a</sup> Bold text indicates bias is significant.

**Table 4: Accuracy associated with LiDAR data, for flat terrain with open sky, where flat is defined as  $\leq 6\%$  slope**

Road Section	Conditions	Error (cm)	Statistic	Error sample (no.)	Bias <sup>a</sup> (cm)
A	Flat ( $\leq 6^\circ$ ) and Open	23	RMSE*(1.96)	85	<b>+7.8</b>
B	Flat ( $\leq 6^\circ$ ) and Open	16	RMSE*(1.96)	48	<b>-2.9</b>

<sup>a</sup> Bold text indicates bias is significant.

**Table 5: Accuracy associated with LiDAR data, for flat terrain with canopy, steep terrain with open sky, and steep terrain with canopy, where flat is defined as  $< 6$ -degree slope, and steep is defined as  $> 25\%$  slope**

Road Section	Conditions	Error (cm)	Statistic	Error sample (no.)	Bias <sup>a</sup> (cm)
A	Flat ( $\leq 6^\circ$ ) with Canopy	34	95 <sup>th</sup> %	32	<b>+16</b>
A	Steep ( $\geq 25^\circ$ ) and Open	49	95 <sup>th</sup> %	26	+7.5
A	Steep ( $\geq 25^\circ$ ) with Canopy	61	95 <sup>th</sup> %	128	<b>-29.0</b>

<sup>a</sup> Bold text indicates bias is significant.

The most certain result from our analysis was that the vendor's accuracy claim of <20 cm RMSE at 95% confidence interval in flat, open, hard areas was valid. When evaluating conditions, for relatively flat terrain that was assumed to have a hard surface, the RMSE at 95% confidence level was 18 cm in Road Section A, and 11 cm in Road Section B (Table 3). Since all errors were obtained by subtracting conventional survey elevations from LiDAR elevations, a positive bias result indicates that the LiDAR elevation was higher than the conventional survey. The bias of 6.4 cm in Road Section A with flat terrain (<3-degree slope) and open sky conditions shows how it is possible to have a significant bias yet still adhere to the RMSE accuracy statement. The fact that in the same terrain conditions in Road Section B, the error bias was -2.4 cm is reassuring because it illustrates that the LiDAR is not consistently overestimating elevation along the study corridor.

The 95<sup>th</sup> percentile statistics showed that, as expected, the worst elevation precision was associated with areas of steep terrain with canopy (61 cm). The next-worst elevation precision was associated with areas of steep terrain and open sky (49 cm) (Table 5), followed by areas of flat terrain with canopy (34 cm) (Table 5). The positive bias of 16 cm associated with flat terrain with canopy was not entirely unexpected (Table 4); it indicates that the ground classification algorithms under canopy tended to misclassify vegetation as ground points, which is a common error in many aerial LiDAR datasets.

An important point about outliers is that they can disproportionately affect statistics. For example, by trimming errors for steep terrain with canopy between -2 and 2 m, the 95<sup>th</sup> percentile error remains relatively unchanged at 62 cm, but the bias reduces to -18 cm. In this case, trimming the data discards many situations in which horizontal error may have contributed to vertical error because obtaining an error measurement required a LiDAR DEM raster cell value that corresponded to the exact position of a conventional survey point. LiDAR horizontal error may have shifted the DEM and caused the analysis to use a raster cell with a different elevation than if the data had been perfectly aligned in the horizontal direction. This partially explains why it is difficult to gather good statistics for steep areas. Regardless, the results are still useful in helping better understand errors in LiDAR data for sloped conditions—as long as the limitations of the statistical tests are also considered.

## **Effects of Post-Survey Breaklines on Earthworks Calculations**

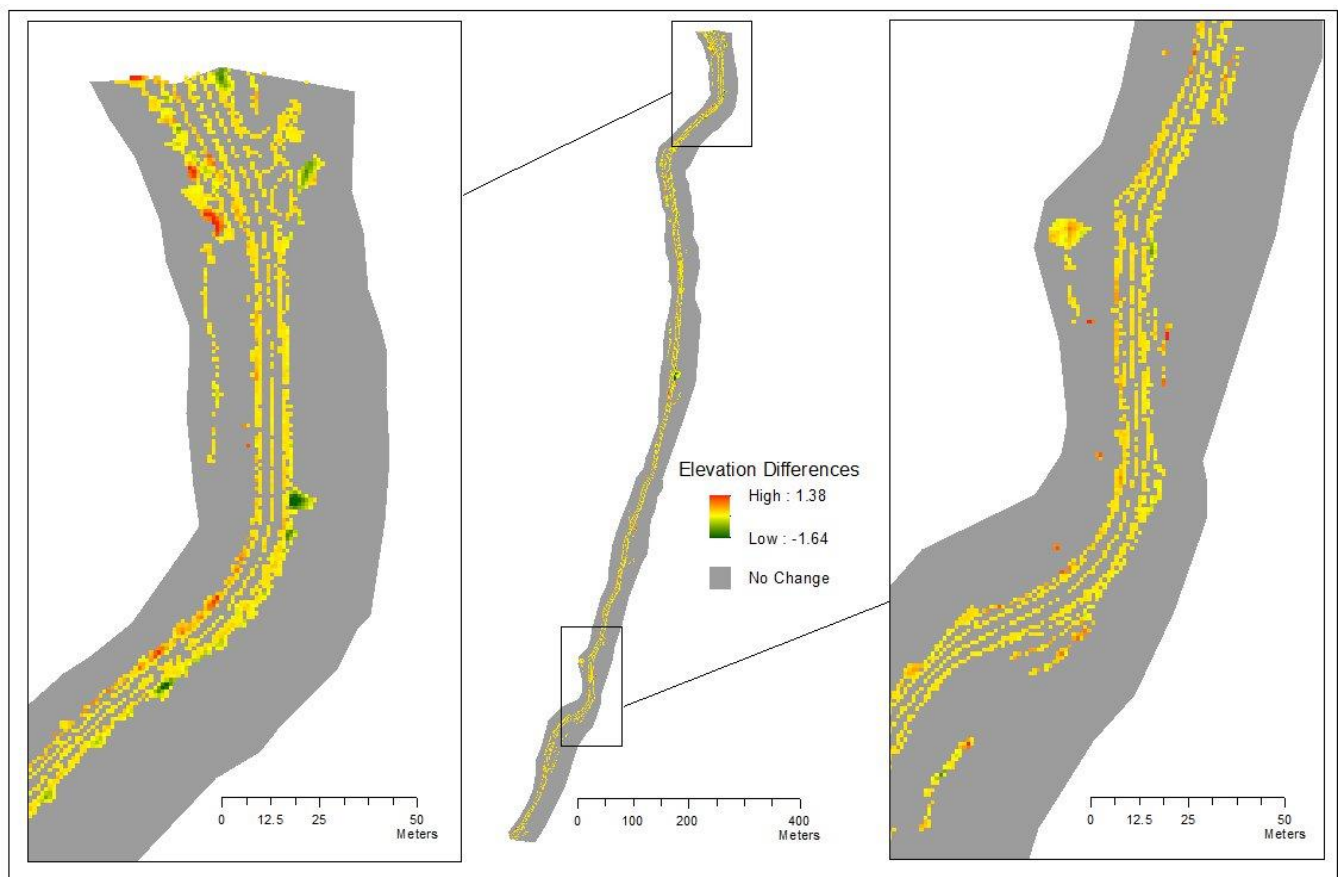
In order to test how post-survey breaklines could affect earthworks calculations, breaklines and LiDAR ground points were used to create a TIN. The TIN was then converted to a raster DEM that aligned with the original supplied DEM derived using LiDAR ground points alone. Using a raster DEM rather than a TIN for earthworks calculations is not a typical approach for a CAD environment such as RoadEng. The advantage to preparing the raster DEM, however, is that in a GIS environment, raster DEMs can be subtracted from one another to produce a visualization of elevation differences.

Figure 17 shows the raster that results when subtracting the cells of the original DEM from the DEM created with the help of breaklines. The analysis found that the average value of all cells that recorded a change in elevation was 0.003 cm. In other words, the negative and positive differences introduced with the breaklines cancelled each other out.

### Summary and Discussion of the Effects of Post-Survey Breaklines in DEM Production

Using the breakline-generated DEM in place of the original DEM produced elevation differences up to 1.64 m locally, but overall the average value of cells that changed value was nearly zero. This suggests that when calculating earthworks for larger areas, such as a typical construction section of 2 km in length, breaklines would not likely have a large effect on predictions of cut-and-fill volume.

Figure 17 highlights elevation overestimations in the original DEM. The large green area at the bottom of the figure is where some deciduous trees were overhanging the road and consequently blocked many LiDAR points from reaching the ground. If this road section had a more overhanging deciduous canopy along it, it is possible that this may have started to create a significant difference between the original DEM and the DEM created with the help of breaklines.



**Figure 17: View of the difference raster for Road Section A. The entire section is shown in the middle and to the left and right are two detail areas. The raster image was created by subtracting original DEM cell values from cell values of DEM created from LiDAR points and post-survey breaklines. The maximum difference of 1.38 m is shown in red, and the minimum difference of -1.64 m is shown in green. Yellow indicates a difference near zero, while grey areas are cell values that did not change.**

## Cut-and-Fill Differences Using LiDAR Versus Conventional Terrain Models

It is challenging to evaluate how the terrain model derived from the LiDAR dataset versus that derived from a conventional ground-survey dataset affects volumetric calculations for road re-alignment because the re-alignment design cannot be identical for both terrain models. Specifically, the problem is that if the terrain model from the conventional survey is simply swapped for the LiDAR-derived model, the slope-stakes delimiting earthworks no longer make sense; therefore either the slope-stakes and/or the road centreline need to be modified.

Onsite Engineering addressed this problem in RoadEng by keeping the same horizontal and vertical coordinates for the centreline and ditch, and modifying the slope-stake positions. This involved meticulously inspecting and adjusting the designs using the cross-section profile views every 5 to 10 m. Figure 18 illustrates that terrain models can be very different if they are created with different slope-stake locations. Onsite Engineering's work is summarized in Table 6 and Table 7.

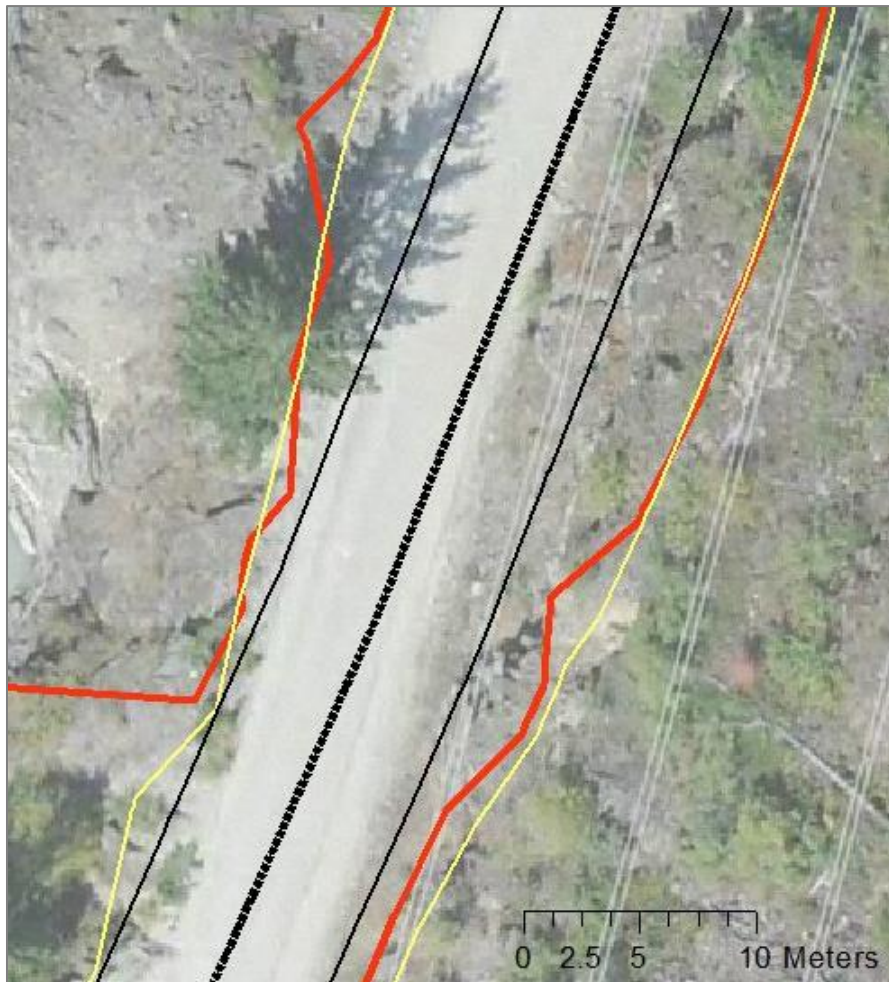


**Figure 18: Example of how slope-stake locations vary according to the ground model. The black lines denote the location of a re-aligned road. Using the same centreline, there are differences between slope stakes associated with a terrain model derived from conventional ground-survey data (yellow line) compared to that derived from the LiDAR survey data (red line).**

**Table 6: Estimated earthworks volumes for Road Sections A and B: a comparison of calculations by model**

Road Section	Element	Type of survey		Difference relative to LiDAR	
		LiDAR (m <sup>3</sup> )	Conventional (m <sup>3</sup> )	(m <sup>3</sup> )	(%)
A <sup>a</sup>	Cut	16,624	19,139	-2,515	-15
	Fill	7,048	5,538	1,510	21
B <sup>b</sup>	Cut	23,552	21,364	2,188	9
	Fill	6,483	5,063	1,420	22

<sup>a</sup> 1.5 km long, complex terrain, total station survey.

<sup>b</sup> 2.24 km long, relatively flat, combination of total station and hand survey.

**Table 7: Estimated earthworks volumes at three road subsections in road section A and section B for which corresponding ground-truthed estimates were available: a comparison of calculations by model**

Road Subsection <sup>b</sup>	Element	Type of survey <sup>a</sup>		
		Detailed total station (m <sup>3</sup> )	LiDAR (m <sup>3</sup> )	Conventional (m <sup>3</sup> )
A1	Cut	860	981	900
	Fill	25	12	58
A2	Cut	403	377	426
	Fill	12	12	24
A3	Cut	199	211	179
	Fill	21	84	14
B1	Cut	389	431	362
	Fill	0	0	0
B2	Cut	307	320	259
	Fill	1	1	1
B3	Cut	2418	2206	1685
	Fill	2	5	7

<sup>a</sup> Green font = best predictor.

<sup>b</sup> See Table 2 for descriptions of each subsection.

### Summary and Discussion for Earthworks Analysis

The methodology used to compare earthworks differences in Road Sections A and B could not acquire ground-truth data, in part, because the road construction had not yet occurred. It would be possible to obtain these data after completion of the re-alignment, but this task would be very difficult to do and prone to error. A major reason is that resource road designs are not always accurately followed at the time of actual construction because previously unknown field conditions are often encountered. If the

road was resurveyed in attempt to get a true picture of post-construction terrain, and to then get true volumes, the original designs would then need to be modified to match the actual re-alignment. Many other assumptions and estimations would also need to be introduced.

Even though this study did not have true volume data to compare to, examining the differences between the two models still provides value. The differences in volumes associated with Road Sections A and B show that, when LiDAR volumes were used as the reference, the maximum magnitude of volumetric differences was approximately 10 to 15% for cut volumes, and 20% for fill volumes (see Table 6). The magnitude of volume differences was roughly equivalent for both sections even though they had differing terrain and appropriately differing conventional survey methods. This suggests that the conventional surveys and associated georeferencing were fairly well executed. Cut volume differences at Road Sections A and B were -15% and 9% respectively (see Table 7), and the difference in signage adds some assurance that using the LiDAR terrain model did not tend to create bias in volume differences. More generally, all of these data provide insight into what kind of differences might be expected in other sections along the In-SHUCK-ch FSR and other similar resource roads.

The detailed total station surveys at the six subsections compensate for the lack of a true elevation values in Road Sections A and B, which would be highly impractical and time consuming to acquire. Results from the subsection analysis show, generally, that the LiDAR surface was at least as good a predictor as the corresponding conventional survey. In Road Subsection B3, the subsection with the most earthworks, the LiDAR was by far the better predictor of earthworks (Table 7), probably because this was a very steep area and the conventional survey acquired few side shots. Predicted volume differences were not as extreme in Road Section A, likely because the conventional survey was much more detailed than in Road Section B.

## OVERALL BENEFITS AND LIMITATIONS OF LIDAR

LiDAR surveys are vastly more efficient to execute than conventional ground surveys but efficiency does not always translate to effectiveness for a given application. In order to evaluate how effective LiDAR was for the In-SHUCK-ch FSR re-alignment project, this study investigated the accuracy of LiDAR in several ways.

The following are some overall observations of the benefits and limitations of LiDAR.

### Benefits

Given that the LiDAR survey

- i) adhered to the LiDAR vendor's stated vertical accuracy,
- ii) performed well in the vertical accuracy assessment in different terrain conditions,
- iii) had relatively minor bias values associated with different terrain conditions,
- iv) had approximately the same magnitude of earthworks differences compared to conventional surveys in Road Sections A and B,
- v) generally performed as well or better than conventional surveys in the subsection volumetric analysis, and
- vi) has millions more points than conventional surveys,

it is reasonable to infer that, for earthworks calculations, the LiDAR dataset led to the creation of a more accurate terrain model than did the dataset from the conventional surveys.

A major advantage of LiDAR is that its accuracy can be readily checked with an RTK system. If there are discrepancies with a ground survey, however, verifying the accuracy of the LiDAR dataset would require costly traverses backwards to close a survey loop, and/or collection of new points to densify the survey. Furthermore, in the interest of cost savings, conventional as-built surveys along roads rarely transverse back to verify accuracy; therefore, the resulting terrain model may include errors that could affect calculations of earthworks volumes. Of the sections that the LiDAR accuracy study tried to georeference, the one on KM 6 did not align, which was suspected to be due to blunders in the ground survey.

Acquiring LiDAR also has planning-level benefits that may be pertinent in a re-alignment project. This situation occurred during the In-SHUCK-ch FSR upgrade project near KM 1. Onsite Engineering was designing an upgrade to a complex road alignment featuring very steep terrain and hydro poles in close proximity to the roadway. Onsite Engineering decided that they would design a temporary road to bypass construction. Since LiDAR was available for 250 m uphill, they immediately spotted what looked like an old road that could be leveraged to construct the temporary road. The cost savings were at least a day or two of field work; although Onsite Engineering still needed to visit the location to verify ground conditions, they already knew where to go. Although harder to quantify, an associated benefit from spending less time in the field is increased safety due to less exposure to hazardous terrain, etc.

## **Limitations**

In general, the major deterrent to LiDAR acquisition is the large, upfront, investment. Collecting aerial LiDAR and imagery for a 74-km-long, 500-m-wide road corridor such as the re-alignment of the In-SHUCK-ch FSR is estimated to cost between \$40,000 and \$70,000, or approximately \$500 to \$1000/km, assuming that the LiDAR vendor's plane is relatively close to the site (i.e., low mobilization costs). In comparison, a ground-based crew using a total station to carry out an as-built survey at a typical density and which extends to 30 m on either side of the road centreline would take weeks and would cost approximately \$225,000, or roughly \$3000/km.

The return on investment from using LiDAR for road surveying would depend on how many kilometres of road FLNRO works on per year. Assuming a relatively conservative 6 km of a 75 km-long FSR needs an as-built survey in a fiscal year, utilizing a conventional survey approach would cost \$18,000, or roughly one-third of the cost to survey the entire length with LiDAR.

Another limitation that LiDAR introduced is dependencies on expensive field equipment to tie-in when it is necessary to either check or extend the LiDAR survey on the ground. To make an accurate tie-in, a surveyor requires an RTK system which costs about \$500/day to rent, or \$40,000 to \$60,000 to purchase. An RTK system also requires about 30 minutes to set up the base station, which may need to be set up at a location that is upwards of a 15 to 30 minute drive from where new survey points need to be collected. Once new points are being collected by the rover unit, however, survey efficiency can be greater than that of conventional methods—as long as canopy does not interfere with GNSS signal locks.

A related issue to the use of RTK for a tie-in is that new points may be horizontally shifted in relation to LiDAR. The horizontal accuracy of LiDAR in the case of the In-SHUCK-ch FSR was  $\leq 0.3$  m RMSE at 68% confidence level, meaning that a shift of around 0.5 m in a local area along the road should not be entirely unexpected. Depending on the importance of the horizontal accuracy, the LiDAR in the area of interest could be shifted to match the ground point observations if enough ground points are collected to discern terrain forms that are also distinguishable in LiDAR. Of course this would also introduce interpretation error, as was already the case in the reported horizontal accuracy because the LiDAR vendor needed to use orthophotos to interpret the centre of a ground target. Vertically adjusting LiDAR is much simpler because it only requires the shifting of all points up or down by the opposite value of the bias found in open and flat areas.

Lack of penetration through the forest canopy is another limitation of LiDAR surveys. The LiDAR dataset for the In-SHUCK-ch FSR included areas where the tree canopy had blocked the LiDAR, resulting in ground hits that were 5 to 10 m apart. Terrain that has deciduous trees and/or dense stands of young trees can be especially susceptible to this. Although the LiDAR data for the In-SHUCK-ch FSR were collected during summer, deciduous tree canopies did not seem to cause much of a problem in the analyzed sections of road, in part because this was not a very common type of vegetation near the road. Post-survey breaklines produced by the LiDAR vendor aimed to reduce this effect near areas with potentially disguisable line features. In this case, these breaklines did affect DEM accuracy locally, but over larger areas changes in elevation caused by the introduction of breaklines averaged to zero. In other locations of coastal British Columbia, acquiring enough LiDAR ground points may be more challenging, especially in areas encompassing vastly different terrain and/or forest.

LiDAR ground misclassification is a related issue. Along the In-SHUCK-ch FSR, accuracy testing in areas of flat terrain with canopy indicated that LiDAR tended to overestimate terrain elevation by 16 cm. This suggests that vegetation may have been misclassified as ground in some instances. While this overestimation was relatively low in this case, it may not always happen that way. The elevation error could vary, depending on the LiDAR collection conditions and forest characteristics, or if the LiDAR vendor alters their proprietary ground point identification algorithms.

An overarching disadvantage of LiDAR is that it presents what could be seen as many technological complications that do not apply to conventional surveying. In terms of field work, this includes dealing with RTK software and the post-processing of collected data, accounting for GNSS constellations that would affect the quality of the rover survey, and adjusting LiDAR to the more accurate RTK survey (if required). Complications to post-processing work will generally revolve around the vast amount of data that LiDAR contains. Older computers may not be able to handle large LiDAR datasets well, and new software may be needed. Data storage may become an issue if the data are replicated so that many different groups can use it.

## CONCLUSIONS

At the request of the British Columbia Ministry of Forests, Lands and Natural Resource Operations (FLNRO), in 2014 FPInnovations studied the accuracy and benefits of using aerial LiDAR as a means of acquiring as-built terrain models to inform upgrade designs of forest resource roads, relative to using conventional ground-based surveys. A LiDAR dataset from the In-SHUCK-ch Forest Service Road (FSR), located in the coastal mountains east–northeast of Vancouver, British Columbia, was used as a case study.

FPInnovations examined the LiDAR vendor’s deliverables by reviewing the types of data produced, the implemented field methods, and the details of the various accuracy reporting techniques. A field study was then designed and executed to georeference existing conventional surveys in order to gain understanding of the errors of the LiDAR-based terrain model and of how these affect earthworks estimations in road re-alignment designs.

Using georeferenced conventional ground surveys for two parts of the FSR, i.e., Road Section A and B, the LiDAR vendor’s vertical accuracy statement of  $\leq 20$  cm RMSE at a 95% confidence level for any flat, open, hard surfaces was confirmed. In addition, the vertical accuracy was evaluated in Road Section B for flat terrain with canopy, steep terrain with open sky, and steep terrain with canopy. The respective errors using 95<sup>th</sup> percentile reporting were 34 cm, 49 cm, and 61 cm. A significant bias of 16 cm was found for flat terrain with canopy, which was likely an overestimation caused by misclassification of vegetation as terrain by the algorithms applied by the LiDAR vendor. Errors in steep and open sky terrain did not find a significant bias, possibly due to a smaller error sample size, while the bias in steep terrain with canopy was found to be  $-29$  cm and statistically significant. Error statistics for sloped conditions, however, may have been unavoidably influenced by the horizontal error of the LiDAR.

The effect of post-survey breaklines was analyzed in Road Section A. The differences in cell values were up to  $\sim 1.6$  m locally, but overall the average difference was zero. This implies that over larger areas, the elevation differences that result with the inclusion of breaklines tended to cancel out.

The georeferenced conventional ground surveys also informed a comparison of how earthworks predictions are affected when a terrain model derived from ground surveys is swapped for a LiDAR terrain model. Changing the terrain model also required adjustment of the slope-stake design to match updated information. The magnitude of earthworks differences ranged from 9 to 22%, which included negative and positive values, suggesting that there is no consistent bias in the volumetric differences. Since it was not possible to acquire a “true” terrain model for the two road sections, six small subsections of the road were surveyed in extreme detail so that earthworks for these subsections could be calculated. At these subsections, LiDAR performed as well or better than then conventional terrain model.

Overall, the LiDAR survey was concluded as being the better model. While its vertical accuracy may be less compared to conventional surveys, its advantages include that it has a more points, allows for relatively quick accuracy checking, has fairly small bias values under different terrain conditions, and it performed as well or better than conventional surveys in the earthworks analyses. The main limitations of LiDAR are that it can produce sparse ground hits in some conditions, it requires an RTK system for

an accurate tie-in that may end up not exactly aligning with LiDAR, and it can contain some minor bias under different terrain conditions. Perhaps most importantly—LiDAR requires an upfront capital investment.

The price of aerial LiDAR technology has come down recently, which is helping to make it a cost-effective solution for an increasing number of applications. Forestry companies are now beginning to collect LiDAR data over entire tenure areas in order to acquire better terrain models and provide more detailed forest inventory information. In the future, FLNRO may be able to take advantage of this trend to collect LiDAR over its many FSRs as part of an area rather than over just a corridor, thereby reducing the cost of LiDAR acquisition.

## REFERENCES

- American Society for Photogrammetry and Remote Sensing (ASPRS). 2014. ASPRS Positional Accuracy Standards for Digital Geospatial data—Edition 1, Version 1.0, November 2014. *Photogrammetric Engineering & Remote Sensing* 81(3):A1–A26. [online] URL: [http://www.asprs.org/a/society/committees/standards/ASPRS\\_Positional\\_Accuracy\\_Standards\\_Edition\\_1\\_Version100\\_November2014.pdf](http://www.asprs.org/a/society/committees/standards/ASPRS_Positional_Accuracy_Standards_Edition_1_Version100_November2014.pdf)
- ASPRS LiDAR Committee. 2004. ASPRS Guidelines: Vertical Accuracy Reporting for LiDAR Data. Editor, Martin Flood. American Society for Photogrammetry and Remote Sensing (ASPRS), Bethesda, Maryland, USA. [online] URL: [http://www.asprs.org/a/society/committees/standards/Vertical\\_Accuracy\\_Reporting\\_for\\_Lidar\\_Data.pdf](http://www.asprs.org/a/society/committees/standards/Vertical_Accuracy_Reporting_for_Lidar_Data.pdf)
- Congalton, R.G., and Green, K. 2008. *Assessing the Accuracy of Remotely Sensed Data: Principles and Practices*. CRC Press, Taylor and Francis Group, Boca Raton, Florida, USA.
- Federal Geographic Data Committee. 1998. Geospatial Positioning Accuracy Standards—Part 3: National Standard for Spatial Data Accuracy. FGDC-STD-007.3-1998. Subcommittee for Base Cartographic Data, Federal Geographic Data Committee Secretariat, U.S. Geological Survey, Reston, Virginia, USA. [online] URL: <https://www.fgdc.gov/standards/projects/FGDC-standards-projects/accuracy/part3/chapter3>
- GeoBC. 2014. Specifications for LiDAR, Version 2.0. British Columbia Ministry of Forests, Lands, and Natural Resource Operations, Victoria, British Columbia, Canada. [online] URL: [http://geobc.gov.bc.ca/base-mapping/atlas/trim/specs/GeoBC\\_LiDARSpecifications\\_May\\_2013v2.0.pdf](http://geobc.gov.bc.ca/base-mapping/atlas/trim/specs/GeoBC_LiDARSpecifications_May_2013v2.0.pdf)
- Zandbergen, P.A. 2008. Positional Accuracy of Spatial Data: Non-Normal Distributions and a Critique of the National Standard for Spatial Data Accuracy. *Transactions in GIS* 12(1):103–130.



## Head Office

### Pointe-Claire

570, Saint-Jean Blvd  
Pointe-Claire, QC  
Canada H9R 3J9  
T 514 630-4100

### Vancouver

2665 East Mall  
Vancouver, BC.  
Canada V6T 1Z4  
T 604 224-3221

### Québec

319, rue Franquet  
Québec, QC  
Canada G1P 4R4  
T 418 659-2647



OUR NAME IS INNOVATION